University of Nebraska - Lincoln
DigitalCommons@University of Nebraska - Lincoln

Dissertations & Student Research in Computer Electronics & Engineering

Computer & Electronics Engineering, Department of

8-4-2008

SELF-ENCODED SPREAD SPECTRUM SYNCHRONIZATION AND COOPERATIVE DIVERSITY

Kun Hua
University of Nebraska at Lincoln, khua@mail.unomaha.edu

Follow this and additional works at: http://digitalcommons.unl.edu/ceendiss

Part of the Computer Engineering Commons

Hua, Kun, "SELF-ENCODED SPREAD SPECTRUM SYNCHRONIZATION AND COOPERATIVE DIVERSITY" (2008). *Dissertations & Student Research in Computer Electronics & Engineering.* Paper 1.
http://digitalcommons.unl.edu/ceendiss/1

This Article is brought to you for free and open access by the Computer & Electronics Engineering, Department of at DigitalCommons@University of Nebraska - Lincoln. It has been accepted for inclusion in Dissertations & Student Research in Computer Electronics & Engineering by an authorized administrator of DigitalCommons@University of Nebraska - Lincoln.

SELF-ENCODED SPREAD SPECTRUM SYNCHRONIZATION AND COOPERATIVE DIVERSITY

By

Kun Hua

A DISSERTATION

Presented to the Faculty of

The Graduate College at the University of Nebraska

In Partial Fulfillment of the Requirements

For the Degree of Doctor of Philosophy

Major: Engineering

Under the Supervision of Professor Lim Nguyen

Lincoln Nebraska

May. 2008

SELF ENCODED SPREAD SPECTRUM

SYNCHRONIZATION AND COOPERATIVE DIVERSITY

Kun Hua, Ph.D.

University of Nebraska, 2008

Adviser: Lim Nguyen

This dissertation research concerns a novel self-encoded spread spectrum. It provides a feasible practical implementation for random spreading codes. The traditional transmit and receive PN code generators are not needed. Instead, the spreading codes are extracted from the user's information bits itself. Comparing to conventional CDMA, SESS completely abandons the use of pseudo-random spreading codes. The code variability doesn't depend on the spreading length like pseudo-random codes.

But because the self-encoded spreading sequence is random and time varying, data recovery requires that the despreading sequence be identical with the spreading sequence at the start of the transmission. Synchronization is one of the key techniques in SESS which seeks to recover the initial spreading sequence at the receiver without any prior knowledge. It includes two phases: initial acquisition and tracking. We consider initial acquisition as a global optimization problem and employ genetic search algorithm for converging to the global optimization efficiently. In the tracking phase, we use Markov chain analysis to examine the mean tracking time. We can verify them by simulation

results as sequence length $N=8$. By comparing the analytical and simulation results, we can conclude that the Genetic model and Markov chain analysis can describe the process of the synchronization of SESS system reliably. We extended such synchronization model of SESS to longer sequence length as $N=64$ and achieved the shortest synchronization time by setting an optimum threshold. Optimal parameters are also considered to improve the synchronization time.

We also consider incorporating SESS with cooperative diversity technique to achieve spatial diversity gain with the number of relays. We observe the system's stability in highly correlated rayleigh channels as well as in severe fading channels. Meanwhile, we also consider channel coding for time diversity gain (together with the soft decision Viterbi detection in receiver). Notice that we achieve both time diversity and special diversity while maintaining the same average power as the maximum ratio combiner.

Copyright

by

Kun Hua

2008

To my wife Ying Zhang, and my family members, with profound love and appreciation.

Acknowledgments

In my Ph.D. research, many people have helped and encouraged me. The first two individuals who deserve special thanks are Professor Lim Nguyen and Professor Won Mee Jang, my dissertation advisors, for their guidance, support and encouragement throughout the course of my graduate research. I would like to express my deepest appreciation to Professor Nguyen, who, with great intelligence and incredible work ethic, provided me with both intellectual help for the theoretical aspects of my research and instructive help for my simulated work on the synchronization of self-encoded spread spectrum. I am thankful to Professor Jang for broadening my knowledge in the exciting research field of cooperative diversity, and for her sharp scientific intuition, meticulous scholarship and warm heartedness, which have profoundly influenced me. I would also like to thank my committee, Professor Yaoqing Yang, Professor Haifeng Guo, Professor Lisong Xu. Thanks to Professor Yang for encouraging me in rigorous analysis and thought, and sharing with me his expertise in communication networks. Thanks to Professor Guo, for his suggestions, inspirations and the solid foundation of genetic algorithm knowledge. Thanks to Professor Xu for helping me well organize the thesis and for his infectious research enthusiasm.

My association with Professors Nguyen and Jang's research groups has been an invaluable experience for me. I would like to thank my colleagues, past and present, Yan Kong, Sergio Angarita, Wei Zhang, Kim Tae hyung, Puttipong Mahasukhon, Ting Zhou, Honggang Wang, Wei Wang, Dalei Wu, Jiucai Zhang, Haiyan Luo and Sichuan Ma. I

have very fond memories of our stimulating discussions at the group meetings, the days and nights working on experiments, the good humors and the precious friendships.

Especially thanks to Professor Hamid Sharif, who recruited me into UNL CEEN graduate program, for his tremendous helps on my graduate study. And Professor David Y. S. Lou, who introduced UNL to me five years ago in China, helped me to realize the dream of abroad study. I am indebted to Dr. Harvey Siy and Samantha: their sacrificial friendship has made my graduate study in Omaha an extremely enjoyable journey. Finally, I would like to thank my parents for their love and support.

Kun Hua

The University of Nebraska-Lincoln

May, 2008

TABLE OF CONTENTS

Chapter 1. Introduction **1**

1.1 Historical Backgrounds of Spread Spectrum

1.2 Introduction of Cooperative Diversity

1.3 Motivation and Scope of Research

Chapter 2. Self-encoded Spread Spectrum **13**

2.1 Decision Feedback Receiver

2.2 Iterative Receiver

2.3 Self-encoded Multiple Access

2.4 Summary

Chapter 3. Self-encoded Spread Spectrum Synchronization **26**

3.1 Genetic Algerithm SESS Initial Acquisition

3.2 Markov Chain Analysis

3.3 Synchronization

3.4 Summary

Chapter 4. Coded Cooperative Diversity with Spread Spectrum **58**

4.1 Introduction

4.2 Coded Cooperative Diversity System Model

4.3 Coded Cooperative Diversity System Analysis

4.4 Simulation Result

4.5 Summary

Chapter 5. Self-encoded Spread Spectrum with Cooperative Diversity 74

5.1 Introduction

5.2 Cooperative SESS System Model

5.3 Cooperative SESS System Analysis

5.4 Simulation Result

5.5 Summary

Chapter 6. Concluding Remarks and Future Work 89

Appendix A: Examples of Simulink structures of SESS

Appendix B: Mean First Passage Time Matrix Calculation

Appendix C: Variance coefficient Calculation of Correlated Channels

References 100

List of Figures

2.1Structure of self-encoded spread spectrum scheme.

2.2 Self-encoding feedback detection performance, N=1,4,8,16,128,1024

2.3 Comparison of feedback and iteration detection, N=4,8,128,512

2.4 BER performance of iteration detection for iteration 1-4

2.5 Structure of SEMA with decision feedback detection

2.6 Comparison of the BER performance of SEMA for K=1,2,4,8,16 for iteration detection with N=64 and feedback detection.

3.1 Receiver structure for SESS initial acquisition.

3.2 Genetic algorithm procedures

3.3 Initial acquisition time $2L1$ (bits) for $N = 8, 64$.

3.4 Acquisition time $2L1$ (bits) with SNR for $N = 8$.

3.5 Theoretical tracking time $L2$ (bits) SNR for $N = 8$.

3.6 Simulation of tracking time $L2$ (bits) for $N = 8$.

3.7 Theoretical and simulation results of synchronization time $2L1 + L2$ (bits) for $N = 8$ under high SNR.

3.8 Initial acquisition time $2L1$ (bits) for $N = 64$.

3.9 Tracking time $L2$ (bits) for $N = 64$.

3.10 Synchronization time $2L1+L2$ (bits) under different SNR for $N = 64$.

3.11 Initial acquisition time $2L1$ (bits) with parallel correlators for $N = 64$.

3.12 Initial acquisition time 2*L1* (bits) with larger sequence pool for *N* = 64.

3.13 Initial acquisition time 2*L1* (bits) with larger sequence pool for cross-over=90% and mutation=5%

3.14 Synchronization time 2*L1*+*L2* (bits) improvement with parallel correlators and a larger sequence pool for *N* = 64.

4.1 Cooperative diversity structure.

4.2 Cooperative diversity structure with convolutional coding.

4.3 Simulation BER, CCC and MRC, 10 *K* = 20 *K* = 30 *K* =1, 12 *K* = 13 *K* = 1.

4.4 Analytical and simulation BER of MRC.

4.5 Simulation BER of MRC with 10 *K* = 20 *K* = 30 *K* =0.5, 12 *K* = 13 *K* = 0.5, for various correlation values of correlated channel.

4.6 Simulation BER of CCC with 10 *K* = 20 *K* = 30 *K* =0.5, 12 *K* = 13 *K* = 0.5, in correlated channel.

4.7 Simulation BER of MRC with 10 *K* = 20 *K* = 30 *K* = 0.5, 12 *K* = 13 *K* = 0.5, under different bit loss percentage.

4.8 Simulation BER of CCC with 10 *K* = 20 *K* = 30 *K* =0.5, 12 *K* = 13 *K* = 0.5, under different bit loss percentage.

5.1 Cooperative self-encoded spread spectrum structure.

5.2 Simulation BER, SESS-CD (64 chips/bit) and MRC, *K10* = *K*20 = *K*30 = 1*;K*12 = *K*13 = 1.

5.3 Probability density function of exact pdf and is pread approximation, 64

chips/bit, *Eb/No* = 5 and 10 dB

5.4 Simulation BER of SESS-CD, 64 chips/bit.

5.5 Simulation BER of MRC and SESS-CD (64 chips/bit) with $K10 = K20 = K30 = 0.5; K12 = K13 = 0.5$, for various correlation values of correlated channel.

5.6 Simulation BER of MRC and SESS-CD (64 chips/bit) with $K10 = K20 = K30 = 0.5, K12 = K13 = 0.5$, under different bit loss percentage.

CHAPTER 1

Introduction

1.1 Historical Backgrounds of Spread Spectrum

Spread Spectrum (SS) refers to a class of modulation techniques in which the bandwidth of the transmitted signal is much higher than the bandwidth of the information being transmitted. To spread the spectrum, for example, the original signal is multiplied by a known code of much larger bandwidth which is independent of the signal and the receiver can reconstruct this code for synchronous detection.

There are several reasons for the spread spectrum to be used.

1. Spread spectrum increases tolerance to interference and jamming.
2. Spread spectrum lowers the probability of hostile interception by masking the transmitted signal in the background noises.
3. In fading channels, by the use of a RAKE receiver, a spread-spectrum receiver can obtain an important advantage in diversity.
4. More than one user is allowed to access a common communication channel. The choice of spreading codes is critical to reducing multiple-access interference (spreading-code cross-correlations) and multi-path self-interference (spreading code autocorrelation).

Spread spectrum has its origin in the military communication and navigation system

in 1950's [1]. Communication systems that employ spread spectrum to reduce the communicator's detectability and combat the enemy-introduced interference are respectively referred to as low probability of detection (LPD) and anti-jam (AJ) communication systems. In 1949 John Pierce wrote a technical memorandum where he described a multiplexing system in which a common medium carries coded signals that need not be synchronized. This system can be classified as a time-hopping spread spectrum multiple access system [2]. Claude Shannon and Robert Pierce had introduced the basic ideas of CDMA in 1949 by describing the interference averaging effect and the graceful degradation of CDMA [3]. De Rosa-Rogoff defined the direct sequence spread spectrum method and introduced the processing gain equation and noise multiplexing idea in 1950 [3]. Price and Green filed for the anti-multipath RAKE patent [4]: signals arriving over different propagation paths can be resolved by a wideband spread spectrum signal and combined by the RAKE receiver. The near-far problem was first mentioned in 1961 by Magnuski [3].

The cellular spread-spectrum application was suggested by Cooper and Nettleton in 1978 [4]. The first-generation (1G) cellular and cordless telephone networks based on analog frequency modulation (FM) were introduced in 1981. To maximize the capacity in an interference-limited cellular environment, the systems used analog technology based on frequency division multiple access (FDMA) scheme. Examples of first-generation cellular systems were Advanced Mobile Phone System (AMPS) in North America, Nordic Mobile Telephone System (NMT-450) in Europe, and Nippon Telephone and Telegraph (NTT) in Japan, with channel bandwidths of 30 kHz, 25 kHz, and 25 kHz,

respectively.

With the advent of very large scale integration (VLSI) chip designs and increasingly sophisticated microprocessor implementation, the second generation (2G) cellular systems emerged in the 1990s. These systems employed digital modulation techniques and spectrally efficient multiple access schemes, referred to as time division multiple access (TDMA) and code division multiple access (CDMA). Although these systems were more complex than their analog counterparts, they offered certain benefits, such as increased capacity, the implementation of voice and low data rate (facsimile) services, and enhanced authentication capabilities. Well-known examples of the second generation systems include the Europe's TDMA Global System for Mobile communication (GSM); North America's TDMA Interim Standard-54 (IS-54), TDMA IS-136, and CDMA IS-95; and Japan's TDMA Personal Digital Cellular (PDC). Moreover, additional services, such as roaming, security, call forwarding, and messaging, were implemented into the 2G systems. During the 1980s, Qualcomm investigated DS-CDMA techniques, in the form of the narrowband IS-95 standard in July 1993 that let to the commercialization of cellular spread spectrum communications in 1996. Multiuser detection (MUD) has been subject to extensive research since 1986 when Verdu formulated an optimum multiuser detection for the additive white Gaussian noise (AWGN) channel, based on the maximum likelihood sequence estimator (MLSE) [5].

With the development of personal communication services (PCS) in recent years, the third generation (3G) systems are driven by the ever-increasing need for high speed data

transmission with mobile capabilities. The requirements for high data rate, especially packet data transmission, bring new challenges for 3G systems. With substantially enhanced capacity and quality of services, 3G wireless technology can provide users with high speed wireless access to the Internet and multimedia services anytime, anywhere and in any form. 3G system attempts to unify the existing diverse wireless systems into a seamless worldwide radio infrastructure, which will be capable of offering the service of global roaming. A worldwide standard is the International Mobile Telecommunication 2000 (IMT-2000) in 1995. The 3G standard that has been agreed upon for Europe and Japan is known as the Universal Mobile Telecommunications System (UMTS). UMTS is an upgraded version fo the Global System for Mobile Communication (GSM) via the General Packet Radio System (GPRS) or Enhanced Data Rates for GSM Evolution (EDGE). The terrestrial part of UMTS is known as UMTS Terrestrial Radio Access (UTRA). The UTRA standard is a wideband CDMA (WCDMA) technology that features easy integration with the existing GSM protocol. The frequency division duplex (FDD) part of UTRA, which is based on the WCDMA standard, offers very high data rates, up to 2 Mbps. The time division duplex (TDD) part of UTRA is called TD-CDMA. The main global competitor to UMTS standards is CDMA2000, which was developed by Qualcomm in the United States. CDMA2000 can deliver full IMT-2000 capabilities (data rates up to 2 Mbps) in one-third as much spectrum as in WCDMA [50].

The good of 3G mobile cellular systems is to adopt the diverse wireless systems into a seamless universal standard that will facilitate global roaming and provide a wide range of services, including multimedia. The 3G wireless systems will generally support high

speed voice and data services in many different radio propagation environments.

There are three basic spread-spectrum techniques: direct sequencing (DS), frequency hopping (FH) and time hopping (TH) [28]. With direct sequence spreading, the original signal is multiplied by a known pseudo-random code of much larger bandwidth. Pseudo-random appears random, but is actually deterministic, so that the receiver can reconstruct the code for synchronous detection. This pseudo-random code is also called pseudo-noise (PN). With frequency-hopped spreading, the center frequency of the transmitted signal is varied in a pseudo-random pattern. For time hopping (TH), the bursts of signal are initiated at pseudo-random times [29].

Spread spectrum bandwidth expansion can also be obtained by the redundancy from error correcting codes. In a conventional narrow-band communication system, bandwidth expansion is generally an undesired feature. However, in spread spectrum systems high efficiency is achievable by employing low rate channel codes alone for bandwidth expansion. We will refer to spreading by channel codes as combined coding and spreading or code-spreading. A limiting factor, though has been the lack of good low rate codes. Spreading and coding are substitute by a single low rate convolutional code and Viterbi decoder is used at the receiver instead of the conventional despreading detector. However this solution is infeasible for practical application when spreading factor is large due to the complexity of the Viterbi decoder. A scrambling code for users separation is always required.

1.2 Introduction of Cooperative Diversity

The requirement of the new generation wireless communication includes increasing channel capacity and improve the quality of communication. Multi-path fading is one of key difficult factors to fulfill such requirement. To overcome multi-path fading, diversity technique is introduced to duplicate signal samples from the transmitter. Each signal sample passes through independent fading channels, and combined at the receiver. Such techniques include: time diversity, frequency diversity and spatial diversity [53].

In telecommunications, a diversity scheme refers to a method for improving the reliability of a message signal by utilizing two or more communication channels with different characteristics. Diversity plays an important role in combating fading and co-channel interference and avoiding error bursts. It is based on the fact that individual channels experience different levels of fading and interference. Multiple versions of the same signal may be transmitted and/or received and combined in the receiver. Alternatively, a redundant forward error correction code may be added and different parts of the message transmitted over different channels. Diversity techniques may exploit the multipath propagation, resulting in a diversity gain, often measured in decibels.

The following classes of diversity schemes can be identified:

- Time diversity: Multiple versions of the same signal are transmitted at different time instants. Alternatively, a redundant forward error correction code is added and the message is spread in time by means of bit-interleaving before it is transmitted. Thus, error bursts are avoided, which simplifies the error correction.

- Frequency diversity: The signal is transmitted using several frequency channels or spread over a wide spectrum that is affected by frequency-selective fading. For example, microwave radio relays often use several regular wideband radio channels, and one protection channel for automatic use by any faded channel. More recent examples include:
    - OFDM modulation in combination with subcarrier interleaving and forward error correction
    - Spread spectrum, for example frequency hopping or DS-CDMA.

- Space diversity: The signal is transmitted over several different propagation paths. In the case of wired transmission, this can be achieved via multiple wires. In the case of wireless transmission, it can be achieved by antenna diversity using multiple transmitter antennas (transmit diversity) and/or multiple receiving antennas (diversity reception). In the latter case, a diversity combining technique is applied before further signal processing takes place. If the antennas are at far distance, for example at different cellular base station sites or WLAN access points, this is called macrodiversity. If the antennas are at a distance in the order of one wavelength, this is called microdiversity. A special case is phased antenna arrays, which also can be utilized for beamforming, Mutiple Input Multiple output (MIMO) channels and space–time coding (STC).

Among them, spatial diversity is more attractive because it does not require extra time and bandwidth resources and can be combined with other diversity techniques.

Although MIMO has obvious advantages and is gradually accepted by new

generation wireless communication protocols [30], problems still exist: The spatial diversity generally requires more than one separated antenna at the mobile terminal. Unfortunately, this is impractical in wireless cellular system due to the size or hardware complexity of the mobile terminal. To solve this limitation, a new form of spatial diversity called cooperative diversity was proposed by Sendonaris [6-7]. Compared to the spatial MIMO system, the cooperation diversity enables single antenna mobiles in a multi-user receiver.

Cooperative diversity networks are attracting increasing attention as a new and promising diversity technique [31]. Somewhat inspired by multi-antenna systems the technology exploits the fact that around a given terminal, there can be other single-antenna terminals which can be used to enhance diversity by forming a distributed (or virtual) multi-antenna system. Cooperative diversity can achieve a diversity order equal to the number of paths between the source and the destination, and in this sense, they offer similar advantages to any existing diversity technique.

User cooperative diversity was introduced as a way to obtain multiple antenna gains even when each user has only one antenna. Cooperative diversity is defined as a communication technique that achieves a diversity gain by using the combination of the relayed signal and the direct signal. A conventional single hop system uses direct transmission where a receiver decodes the information only based on the direct signal while regarding the relayed signal as interference, whereas the cooperative diversity considers the relayed signal as contribution. That is, cooperative diversity decodes the

information from the combination of two signals. Hence, it can be seen that cooperative diversity is an antenna diversity that uses distributed antennas belonging to each node in a wireless network. It is applicable to sensor or mobile communication networks, where, individual sensors, mobiles, or PDAs communicate with a common base station (BS) or access point (AP).

Results have shown that, even though the inter-user channel is noisy, cooperation leads not only to an increase in capacity for both users but also to a more robust system, where users' achievable rates are less susceptible to channel variations. The mobile radio channel suffers from fading, implying that, within the duration of any given call, mobile users go through severe variations in signal attenuation. By effectively transmitting or processing independently fading copies of the signal, diversity is a method for directly combating the effects of fading.

Cooperative diversity was originally proposed as multiple transmitters cooperate by repeating detected symbols of the others, thereby forming a repetition code with spatial diversity [6-7]. These ideas have led to more sophisticated cooperative coding techniques [8] along with forms of cooperative diversity other than coding. For example, network coding fuses data received along multiple routes to increase network capacity [9-11].

There are three different cooperative methods [32]:

1. Amplify-and-Forward, AF

- The user (relay) receives a noisy version of the signal transmitted by the

partner (source).

- The noisy signal is simply amplified and retransmitted.

2. Decode-and-Forward, DF

- The user (relay) attempts to detect the partner's bits (source) and then retransmits the detected bits.
- The partner has to be assigned mutually by the base station.

3. Coded Cooperation , CC

- This method integrates cooperation into channel coding.
- It sends different portions of each user's code word via two independent fading paths.
- Each user tries to transmit incremental redundancy for its partner.

It is noteworthy that cooperative diversity can increase the diversity gain at the cost of lossing the wireless resource such as frequency, time and power resources for the relaying phase. Wireless resources are wasted since the relay node uses wireless resources to relay the signal from the source to the destination node. Hence, it is important to note that there is trade-off between diversity gain and spectrum resource in cooperative diversity.

1.3 Motivation and Scope of Research

This dissertation research concerns a novel self-encoded spread spectrum (SESS) which is first proposed in [12]. It provides a feasible practical implementation for random

spreading codes. The traditional transmit and receive PN code generators are not needed. Instead, the spreading codes are extracted from the user's information bits itself. Comparing to conventional CDMA, SESS completely abandons the use of pseudo-random (PN) spreading codes. The code variability does not depend on the spreading length like PN codes [51]. In this dissertation, we will study the synchronization of SESS and the BER performance of the coded cooperative SESS system.

Because the self-encoded spreading sequence is random and time varying, data recovery requires that the despreading sequence be identical with the spreading sequence at the start of the transmission. We consider SESS synchronization which seeks to recover the initial spreading sequence at the receiver without any prior knowledge. It includes two phases: initial acquisition and tracking. We consider initial acquisition as a global optimization problem and employ genetic search algorithm for converging to the global optimization efficiently [14]. In the tracking phase, we use Markov chain analysis to examine the mean tracking time. By comparing the analytical and simulation results, we conclude that the Genetic model and Markov chain analysis can describe the process of SESS synchronization reliably.

We also consider incorporating SESS with cooperative diversity technique to achieve spatial diversity gain with the number of relays. We observe the system’s stability in highly correlated rayleigh channels as well as in severe fading channels. Meanwhile, we also consider channel coding for time diversity gain (together with the soft decision Viterbi detection in receiver). Notice that we achieve both time diversity and special

diversity while maintaining the same average power as the maximum ratio combiner (MRC).

The dissertation is organized as follow: In chapter 2, we introduce the structure of SESS modulation. Iterative detection and self-encoded multiple access are discussed in detail. In chapter 3, SESS synchronization is studied by a genetic model and a Markov chain analysis. In chapter 4, cooperative diversity with convolutional coding and Viterbi detection are studied for a fading channel. SESS cooperative diversity scheme with iterative detection is introduced in chapter 5. Finally, future works and some concluding remarks are given in chapter 6.

CHAPTER 2

Self-encoded Spread Spectrum

In CDMA communications, each user is assigned a unique PN spreading sequence that has a low cross correlation with other users' sequences [15]. This deterministic sequence has random-like properties with the low cross correlations that are critical for achieving good system performance. A fundamental problem with the deterministic PN codes is that they can be duplicated, potentially compromising the transmission security.

SESS is a novel spread spectrum technique that does not use PN codes. The new technique is unique in that traditional transmit and receive PN code generators are not needed. The transmission security is enhanced not only due to the spread spectrum nature of the signal, but also from the stochastic nature of the unique spectrum spreading and de-spreading processes [33]. As a result, data recovery by an unintended receiver is practically impossible, resulting in ideally secure transmissions. The proposed techniques provide a feasible implementation of random-coded spread spectrum systems that previously have been thought to be impractical. In this chapter, we introduce the basics of SESS communication systems. The BER performance of the decision feedback receiver is analyzed in section 2.1. Iterative detection is analyzed and compared with the feedback detection in section 2.2. Self-encoded multiple access is considered in section 2.3.

2.1 Feedback Detection

Figure 2.1 shows the block diagram of direct sequence SESS. The spreading code is obtained from the random digital information source itself. At the transmitter, the delay registers are constantly updated from an *N*-tap, serial delay of the data, where *N* is the code length. The current bit is spread by the time varying, *N* chip sequence that has been obtained from the previous *N* data bits. The random nature of the digital information source is assured by applying appropriate data compression methods to remove any redundancy in the data stream, thereby maximizing its entropy. The binary data symbols therefore can be modeled as independent and identically distributed Bernoulli random variables. Symbol values of +1 and -1 occur equally likely with a probability of 1/2. As a result, the spreading sequence is not only randomly generated and independent of the current symbol, but also dynamically changing from one symbol to the next. This smoothes out the spectrum of the signals and eliminates the spectral lines associated with PN sequences [16].

The self encoding operation at the transmitter is reversed at the receiver [55]. The recovered data are fed back to the *N*-tap delay registers that provide an estimate of the transmitter's spreading codes required for signal de-spreading. Data recovery is by means of a correlation detector. Notice that the contents of the delay registers in the transmitter and receiver should be identical at the start of the transmission. This is accomplished as part of the initial synchronization procedure. Unless initially

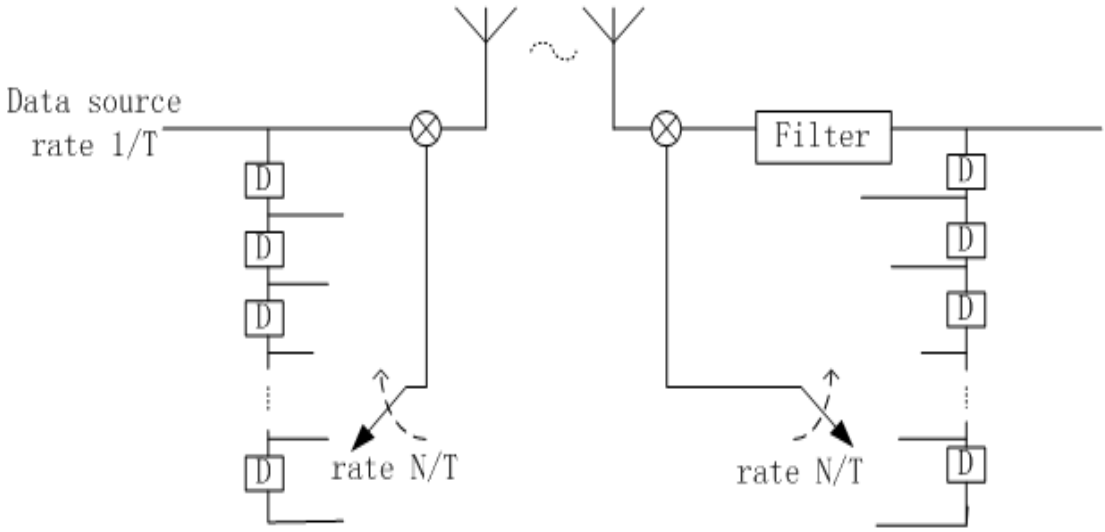

Figure 2.1 Structure of self-encoded spread spectrum scheme.

synchronized and having a complete knowledge of the tap register structure (intended receiver), data recovery will be extremely unreliable since the spreading codes as constructed are time-varying, random, and uncorrelated. As a result, self encoding makes data recovery by an unintended receiver practically impossible.

Figure 2.2 shows the BER performance of the feedback detector. The plots show that self interference causes a performance degradation compared to BPSK modulation at low *SNR* (< 4dB). Also at low *SNR* region, the BER performance degrades as *N* decreases. The degradation is caused by error propagation such that each detection error contributes to a larger attenuation of the signal strength for smaller values of *N*. The effect of self interference is reduced as the spreading length increases, and is practically eliminated for *N*>64.

2.2 Iterative Receiver

We can write the transmitted SESS signals as:

$$\begin{aligned}
s_1 &= b_0b_1, \quad b_{-1}b_1, \quad \ldots\ b_{-N+1}b_1 \\
s_2 &= b_1b_2, \quad b_0b_2, \quad \ldots\ b_{-N+2}b_2 \\
s_3 &= b_2b_3, \quad b_1b_3, \quad \ldots\ b_{-N+3}b_3 \\
&\ldots \\
s_N &= b_{N-1}b_N, \quad b_{N-2}b_N, \quad \ldots\ b_0b_N \\
s_{N+1} &= b_Nb_{N+1}, \quad b_{N-1}b_{N+1}, \quad \ldots\ b_1b_{N+1}
\end{aligned} \tag{2.1}$$

where b_i is the data bit. Since the current bit is spread by *N* previous bits, we can observe that current detecting bits b_i is spread by *N* previous symbols $b_{i-1\ldots}b_{i-N}$ at a rate *N/T*. From

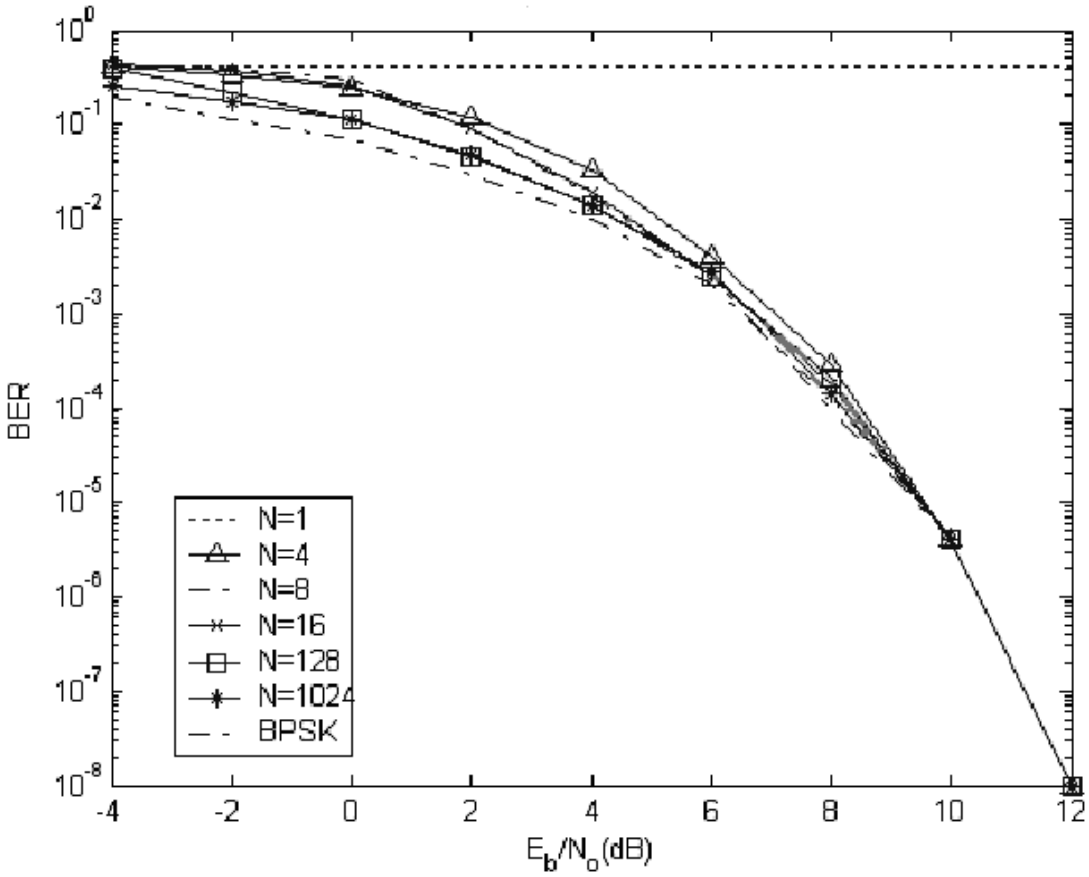

Figure 2.2 Self-encoding feedback detection performance.

the above equations, we can see, for example, the current detecting bit b_1 is not only modulated by the previous N information bits, which are stored in the delay shift register $b_{-N+1...}b_0$, but also appears in N future transmitted signals $s_2,\ldots, s_{N+1}$: there is one chip in each N future transmitted signal, $s_2,\ldots, s_{N+1}$, that contains the information about b_1. By incorporating future transmitted signals together with previous detected bits, we expect to improve the performance over the feedback detector, which only estimates the current bits by correlating with N previous detected bits [56].

Figure 2.3 compares the BER performance of the feedback and iterative detectors, for N=4,8,128,512. A 3dB performance gain can be achieved by the iterative detectors. This is because iterative detection not only uses the last N-bits sequence to achieve data in receiver, but also employs N future sequences for decoding decision: the detector SNR is thereby doubled.

Figure 2.4 shows the BER performance by the iterative detector with iteration from 1 to 4. The BER improves some what as the number of iteration increases, especially at moderate *SNR* from 0dB to 4dB, the errors are more likely to be corrected by re-estimates with additional iterations. The most improvement in terms of BER is achieved with iteration 1 and 2. But limited performance gain is achieved by the number of iteration higher than 2. Iterative detector can achieve a 3dB gain compare to BPSK performance which is the upper bound curve.

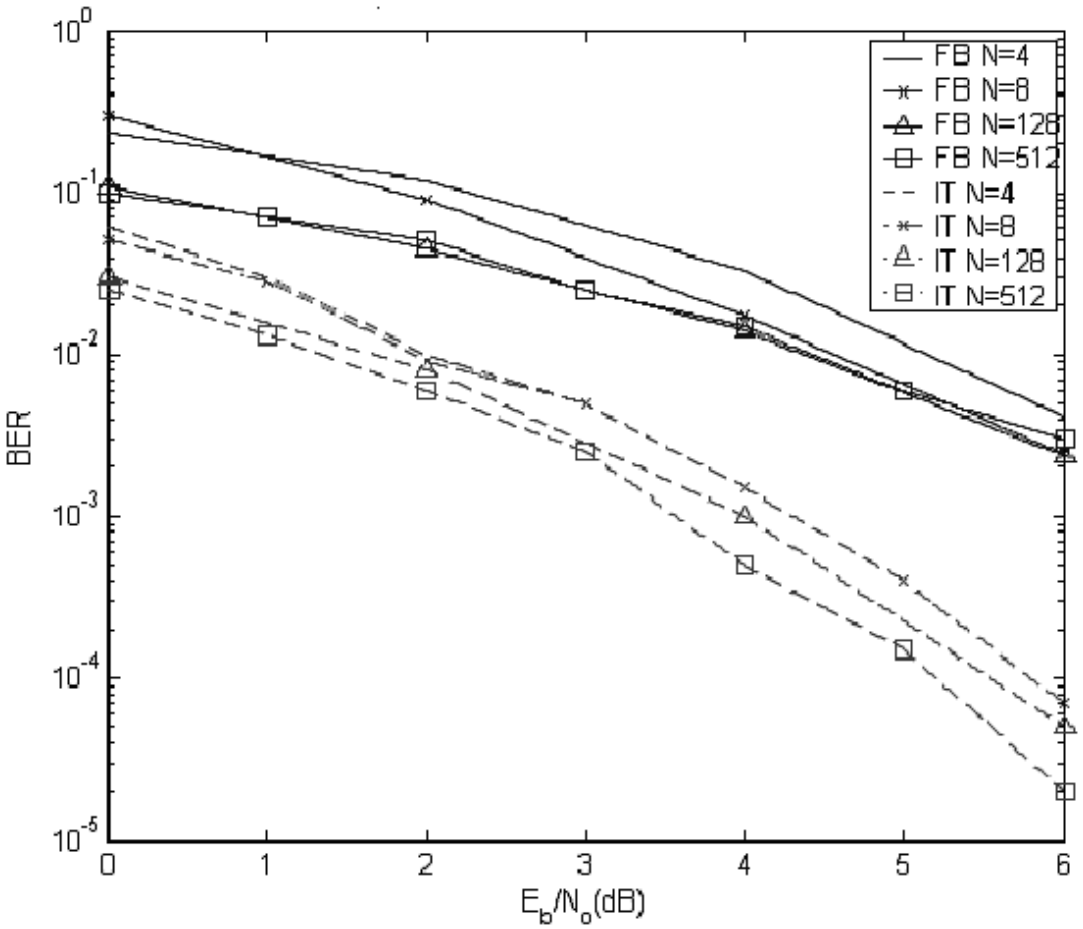

Figure 2.3 Comparison of feedback and iteration detectors.

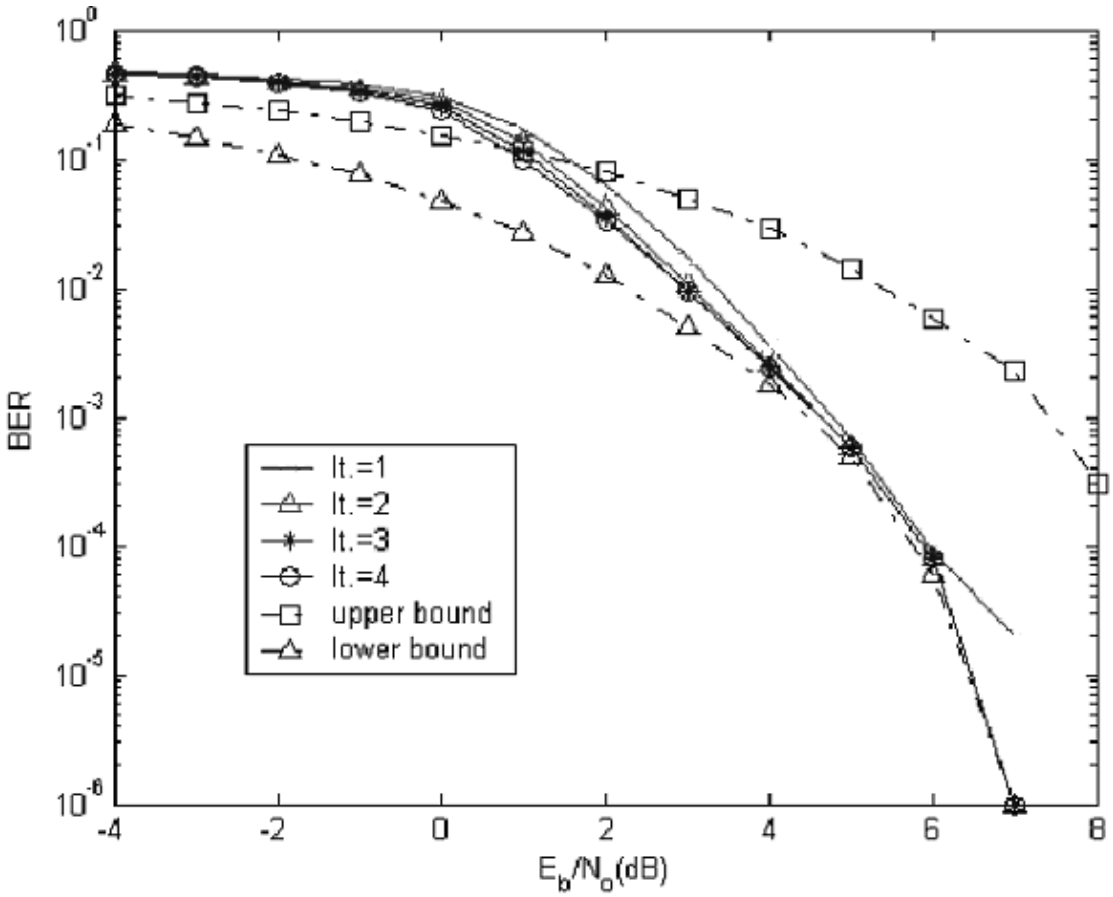

Figure 2.4 BER performance of iteration detector from Iteration 1-4 iterations

2.3 Self-Encoded Multiple Access

The classical way of thinking about communication is considering the signaling between a transmitter in one place and a receiver somewhere else. If there is more than one transmitter or more than one receiver involving in the signaling, this is called multiuser or multiple access communications [57]. Nowadays multiple access communication are widely used in wireless communications to allow many mobile users to share a finite amount of radio spectrum at the same time.

Figure 2.5 illustrates the self encoded multiple access system. Bandwidth expansion is achieved using SESS modulation for each individual user, producing N encoded chips per information bit. These chips are then transmitted over mobile radio channel to the receiver. SESS signals from other users (MAI) are added, producing the resulting received signal [52]. Unlike code spreading CDMA system, where long PN scrambling sequences are required for user separation, SEMA do not require additional PN codes. The self-encoded structure not only spread the information bits but also separates signals from the individual users. Note that SEMA is different from random spreading system in that the users' spreading sequences are not only random, but also changing dynamically from symbol to symbol.

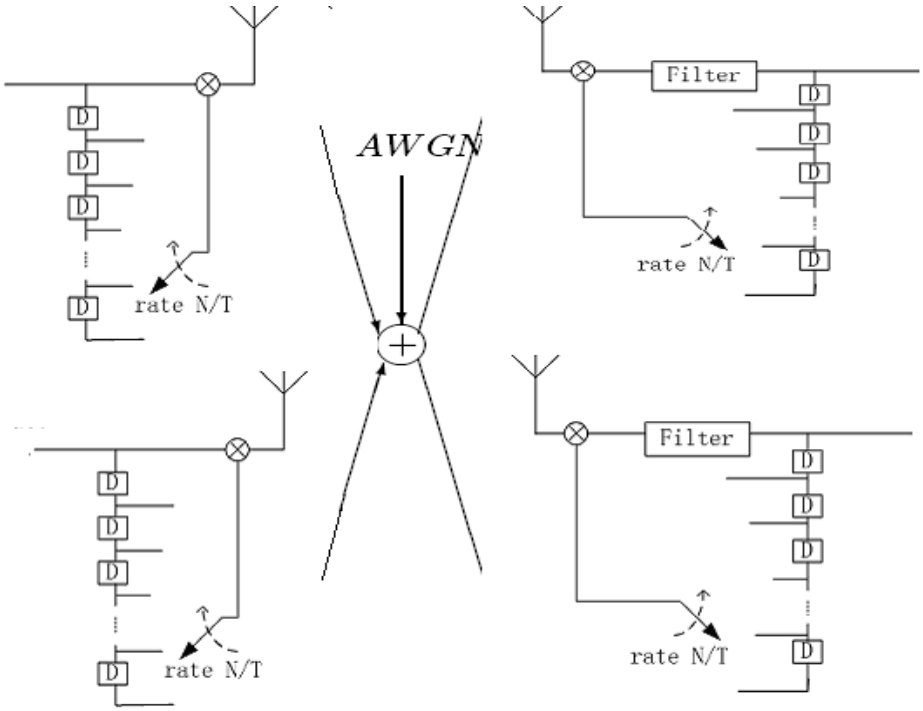

Figure 2.5 Structure of SEMA with decision feedback detection

Severe MAI and error propagation in SEMA receivers may cause the despreading sequences to be mismatched with spreading sequences [58]. In the multiuser case, mismatch of the spreading sequences also results in crosstalk, where unintended signals are received by the desired receiver. When crosstalks occur, the despreading sequence of the desired receiver may correlate better to other users' spreading sequences [59]: the desired receiver then will detect the unintended signal instead. Due to self encoding, the desired receiver may continue to detect the unintended signals from other users.

Figure 2.6 shows the BER performance of iterative and feedback detectors with N=64. The plots show that the BER degrades gradually as the number of users increases. For K>1, the gain of the iterative detector is less than 3dB due to error propagation and MAI. The results also show that Iterative detector can improve the multi-user performance.

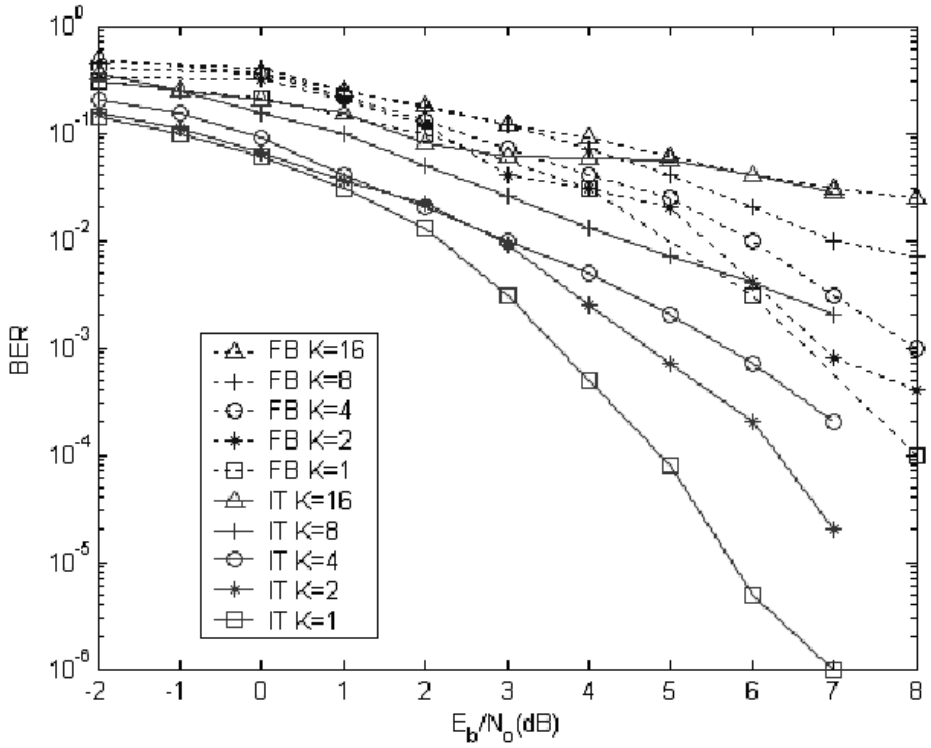

Figure 2.6 Comparison of the BER performance of SEMA for K=1,2,4,8,16 for iteration detection with N=64 and feedback detection.

2.4 Summary

In this chapter, we introduced the structure of SESS system. We investigated the performance of the decision feedback correlation receiver for SESS, and compared it with the iterative detector. Iterative detector provided a 3dB performance gain at high SNR compared to the feedback detector. The detectors were also analyzed for multiple access channel with AWGN noise. The BER performance of SEMA is improved by iterative detection which exploits the data redundancy of SEMA signals to mitigate MAI.

CHAPTER 3

Synchronization of Self-Encoded Spread Spectrum

In traditional spread spectrum communication, the deterministic PN code is known by both the transmitter and receiver [34,35]. The receiver regenerates the code locally and phase synchronization is set up by a partial correlation over a length of the known spreading codes. If the correlation threshold is exceeded, the de-spreading and spreading sequences are assumed to align and code synchronization is declared [13,15,17,18].

However, in SESS the self-encoded spreading sequence is random and time varying. An exhaustive optimum acquisition of an initial random spreading sequence of length N requires that 2^N sequences be generated and searched. Clearly, this is impractical.

In this chapter, we consider SESS synchronization which seeks to recover the initial spreading sequence at the receiver without any prior knowledge [22]. It includes two phases: initial acquisition and tracking. Initial acquisition is achieved when the transmitter spreading sequence has been reproduced at the receiver to within an acceptable number of initial chip errors. This requires that the receiver performs a random search over a vast possible solutions set. Thus, initial acquisition can be considered as a global optimization problem. We propose to employ genetic search algorithm (GA) in the sequence generation and revision for converging to the global optimization efficiently. The search ends when the generated sequence matches with the received sequence with no more than a specified number of chip errors m. In the

tracking phase, the detected chip errors in the receiver delay register transits from the initial state of *m* errors into the error-free state. The mean tracking time can be examined via Markov chain analysis.

In section 3.1, we describe the genetic algorithm acquisition phase. Section 3.2 analyzes the tracking phase using Markov chain. The over all synchronization time performance is analyzed in section 3.3.

3.1 Genetic Algorithm in Initial Acquisition

Initial acquisition in SESS can be considered an unconstrained optimization problem. Finding the global optimization by searching over the entire solution set is the subject of deterministic methods like tunneling method, covering method, zooming method, etc. These methods find the global minimum by means of an exhaustive search. For instance, the basic idea of the covering method is to cover the feasible solution set by evaluating the objective function at all points. These algorithms have high reliability and accuracy is always guaranteed, but they have a slow convergence rate [19].

Given the exponential size of our solutions set, we need an efficient algorithm with a high reliability and fast convergence rate. Many stochastic optimization algorithms have been proposed such as simulated annealing, ant colony, genetic algorithm, etc. GA has proven to be the most powerful and successful one for a wide range of applications, that strikes a balance between reliability and convergence rate.

Genetic algorithm is a search technique used in computing to find exact or approximate solutions to optimization and search problems. Genetic algorithms are categorized as global search heuristics.They belong to a particular class of evolutionary algorithms (also known as evolutionary computation) that use techniques inspired by evolutionary biology such as inheritance, mutation, selection, and crossover (also called recombination).

Computer simulations of evolution started as early as in 1954 with the work of Nils Aall Barricelli, who was using the computer at the Institute for Advanced Study in Princeton, New Jersey. His 1954 publication was not widely noticed. Starting in 1957, the Australian quantitative geneticist Alex Fraser published a series of papers on simulation of artificial selection of organisms with multiple loci controlling a measurable trait. From these beginnings, computer simulation of evolution by biologists became more common in the early 1960s, and the methods were described in books by Fraser and Burnell (1970) and Crosby (1973). Fraser's simulations included all of the essential elements of modern genetic algorithms. In addition, Hans Bremermann published a series of papers in the 1960s that also adopted a population of solution to optimization problems, undergoing recombination, mutation, and selection. Bremermann's research also included the elements of modern genetic algorithms. Other noteworthy early pioneers include Richard Friedberg, George Friedman, and Michael Conrad. Many early papers are reprinted by Fogel (1998).

Although Barricelli, in work he reported in 1963, had simulated the evolution of ability to play a simple game, artificial evolution became a widely recognized

optimization method as a result of the work of Ingo Rechenberg and Hans-Paul Schwefel in the 1960s and early 1970s - his group was able to solve complex engineering problems through evolution strategies. Another approach was the evolutionary programming technique of Lawrence J. Fogel, which was proposed for generating artificial intelligence. Evolutionary programming originally used finite state machines for predicting environments, and used variation and selection to optimize the predictive logics. Genetic algorithms in particular became popular through the work of John Holland in the early 1970s, and particularly his book *Adaptation in Natural and Artificial Systems* (1975). His work originated with studies of cellular automata, conducted by Holland and his students at the University of Michigan. Holland introduced a formalized framework for predicting the quality of the next generation, known as Holland's Schema Theorem. Research in GAs remained largely theoretical until the mid-1980s, when The First International Conference on Genetic Algorithms was held in Pittsburgh, Pennsylvania.

As academic interest grew, the dramatic increase in desktop computational power allowed for practical application of the new technique. In the late 1980s, General Electric started selling the world's first genetic algorithm product, a mainframe-based toolkit designed for industrial processes. In 1989, Axcelis, Inc. released Evolver, the world's second GA product and the first for desktop computers. The New York Times technology writer John Markoff wrote[13] about Evolver in 1990.

Genetic algorithms are implemented as a computer simulation in which a population of abstract representations (called chromosomes) of candidate solutions to an optimization problem evolves toward better solutions. Traditionally, solutions are

represented in binary as strings of 0s and 1s, but other encodings are also possible. The evolution usually starts from a population of randomly generated individuals. In each generation, the fitness of every individual in the population is evaluated; multiple individuals are stochastically selected from the current population (based on their fitness), and modified (recombined and possibly randomly mutated) to form a new population. The new population is then used in the next iteration of the algorithm. Commonly, the algorithm terminates when either a maximum number of generations has been produced, or a satisfactory fitness level has been reached for the population. If the algorithm has terminated due to a maximum number of generations, a satisfactory solution may or may not have been reached.

Genetic algorithms find application in bioinformatics, phylogenetics, computer science, engineering, economics, chemistry, manufacturing, mathematics, physics and other fields.

A typical genetic algorithm requires two things to be defined:

1. A genetic representation of the solution domain,
2. A fitness function to evaluate the solution domain.

A standard representation of the solution is as an array of bits. Arrays of other types and structures can be used in essentially the same way. The main property that makes these genetic representations convenient is that their parts are easily aligned due to their fixed size, that facilitates simple crossover operation. Variable length representations may also be used, but crossover implementation is more complex in this case. Tree-like

representations are explored in genetic programming and graph-form representations are explored in evolutionary programming.

The fitness function is defined over the genetic representation and measures the quality of the represented solution. The fitness function is always problem dependent. For instance, in the knapsack problem we want to maximize the total value of objects that we can put in a knapsack of some fixed capacity. A representation of a solution might be an array of bits, where each bit represents a different object, and the value of the bit (0 or 1) represents whether or not the object is in the knapsack. Not every such representation is valid, as the size of objects may exceed the capacity of the knapsack. The *fitness* of the solution is the sum of values of all objects in the knapsack if the representation is valid, or 0 otherwise. In some problems, it is hard or even impossible to define the fitness expression; in these cases, interactive genetic algorithms are used.

Once we have the genetic representation and the fitness function defined, GA proceeds to initialize a population of solutions randomly, then improve it through repetitive application of mutation, crossover, inversion and selection operators.

Initially many individual solutions are randomly generated to form an initial population. The population size depends on the nature of the problem, but typically contains several hundreds or thousands of possible solutions. Traditionally, the population is generated randomly, covering the entire range of possible solutions (the search space). Occasionally, the solutions may be "seeded" in areas where optimal solutions are likely to be found. During each successive generation, a proportion of the existing population is selected to breed a new generation. Individual solutions are selected through a

fitness-based process, where fitter solutions (as measured by a fitness function) are typically more likely to be selected. Certain selection methods rate the fitness of each solution and preferentially select the best solutions. Other methods rate only a random sample of the population, as this process may be very time-consuming. Most functions are stochastic and designed so that a small proportion of less fit solutions are selected. This helps keep the diversity of the population large, preventing premature convergence on poor solutions. Popular and well-studied selection methods include roulette wheel selection and tournament selection.The next step is to generate a second generation population of solutions from those selected through genetic operators: crossover, and (or) mutation.

For each new solution to be produced, a pair of "parent" solutions is selected for breeding from the pool selected previously. By producing a "child" solution using the above methods of crossover and mutation, a new solution is created which typically shares many of the characteristics of its "parents". New parents are selected for each child, and the process continues until a new population of solutions of appropriate size is generated.These processes ultimately result in the next generation population of chromosomes that is different from the initial generation. Generally the average fitness will have increased by this procedure for the population, since only the best organisms from the first generation are selected for breeding, along with a small proportion of less fit solutions, for reasons already mentioned above. This generational process is repeated until a termination condition has been reached.

Standard Genetic Algorithm Procedure:

1. Choose initial population
2. Evaluate the fitness of each individual in the population
3. Repeat:
    1) Select best-ranking individuals to reproduce
    2) Breed new generation through crossover and mutation (genetic operations) and give birth to offspring
    3) Evaluate the individual fitnesses of the offspring
    4) Replace worst ranked part of population with offspring
4. Until termination

Figure 3.1 illustrates the proposed GA acquisition. The received sequence is correlated to the sequences generated and revised in a genetic pool. The search converges when a generated sequence matches with the received sequence with no more than a specified number of chip errors m. In practice, the matching is determined by selecting an appropriate value of threshold at the correlator output.

Figure 3.2 shows the procedure of genetic algorithm in GA pool. The main characteristics of the GA pool are described as follows.

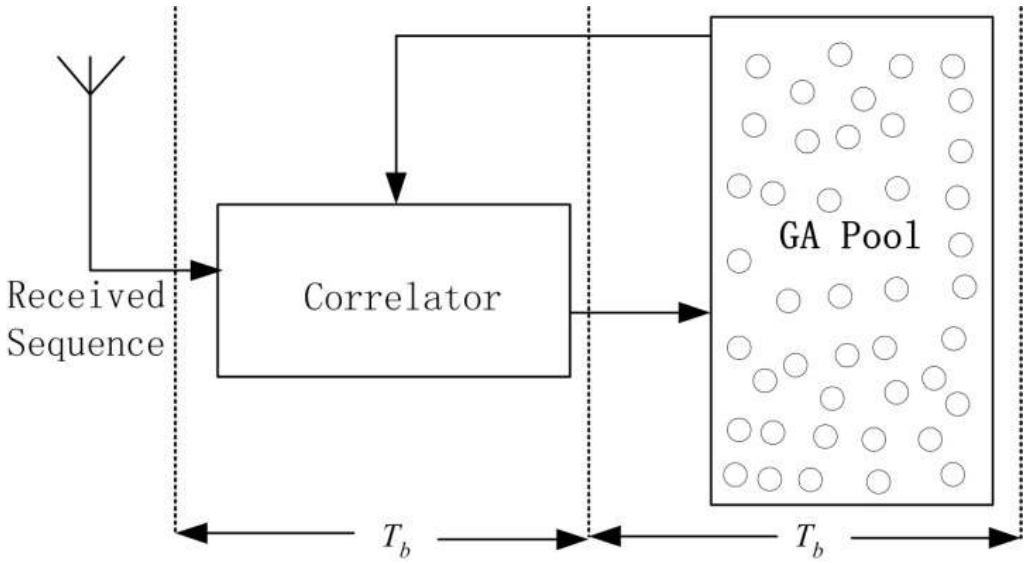

Fig. 3.1 Receiver structure for SESS initial acquisition.

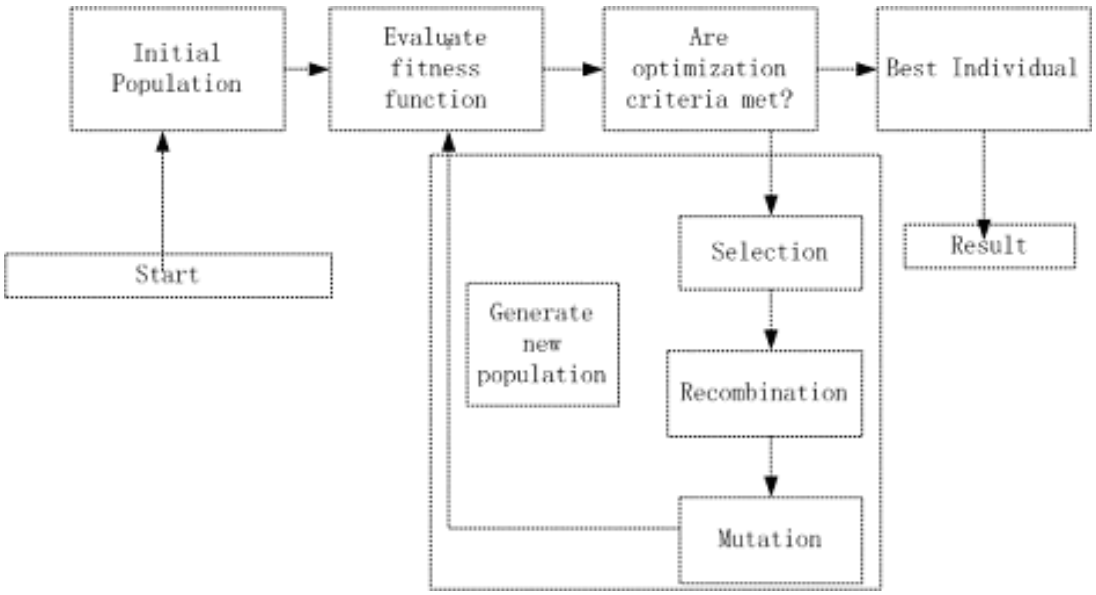

Fig. 3.2 Genetic Algorithm Procedures

1. Initial population: The initial chromosome population is randomly selected from the solution space. In our genetic algorithm, string chromosomes are candidate sequences generated in the GA pool. They are fed back to the correlator bank.

2. Fitness evaluation: The cost function for fitness evaluation is the cross correlations between string chromosomes and received sequence. A higher cross correlation value means that the string chromosome is a better match to the received sequence. The GA pool will keep eugenic chromosomes by maximizing the cost function and eliminate dysgenic ones.

3. Population size: In a GA pool, a larger population size will cover a larger region of solution and increase the reliability for converging to the global maximum. However, this leads to a low searching efficiency because there would be too many chromosomes in the pool. There is a trade off and the population size has typically been chosen to be in the range from 30 to 130 [19]. In our simulation, the population size S is chosen to be 100.

4. Cross-over: Cross-over determines how candidate sequences are updated. Without loss of generality, we choose single point cross-over to simplify the calculation at first, and then increase the percentage in some range. Notice that 95% crossover and 5% mutation are typical [27].

The crossover processing time T_{cr} of the length N sequence in GA pool is taken to be equal to the bit period T_b. The average number of genetic generations L_1 to achieve this

initial acquisition is generally a function of the sequence length N, acquisition chip errors m, and the signal to noise ratio SNR. Under high SNR, L_1 would only depend on N, and m.

With single point crossover and given that there are i chips already matched, subsequent GA search should yield incremental improvement in the number of matching chip, i+1, i+2……matches, until N - m chips are matched. Now assuming that there are already i matched chips between the received and GA-generated sequences, subsequent GA search then should yield incremental improvement in the number of matching chips, until N - m chips are matched. Let T_i be the mean time to achieve $i+1$ matching chips from i matching chips, p_i be the probability for a successful crossover, and k be the consecutive crossover failures before a successful one. T_i is then given by:

$$T_i = T_{cr} \sum_{k=0}^{\infty} (k+1)(1-p_i)^k p_i = \frac{N}{N-i} T_{cr} \tag{3.1}$$

where $p_i = (N-i)/N$. L_1 can be calculated as:

$$\begin{aligned} L_1 &= \frac{1}{T_{cr}} \sum_{j=0}^{N-m-1} \left(\sum_{i=j}^{N-m-1} T_i \cdot \frac{\binom{N}{j}}{2^N} \right) \\ &= \sum_{j=0}^{N-m-1} [(\sum_{i=j}^{N-m-1} \frac{N}{N-i}) \cdot (\frac{N!}{2^N (N-j)!\, j!})] \end{aligned} \tag{3.2}$$

In (3.2), $\sum_{i=j}^{N-m-1} T_i$ represents the overall mean time to achieve N - m matching chips from j matching chips, where j is distributed from 0 to N– m –1 with probability $\binom{N}{j}/2^N$.

The mean acquisition time T is directly proportional to L_1:

$$T = L_1 \cdot (T_b + T_{cr}) = L_1 \cdot (T_b + T_b) = 2L_1 \cdot T_b \qquad (3.3)$$

Equation (3.3) suggests that the mean acquisition time in terms of the number of bits is equal to $2L_1$.

Figure 3.3 plots the example calculations of $2L_1$ for N equal 8 and 64. The results show that the acquisition time decreases as m increases. Notice that for the same fractional chip error of 0.125 (m equals to 1 and 8 for N equals to 8 and 64, respectively), the acquisition time increases significantly, from about 60 bits to about 170 bits as N increases from 8 to 64.

3.2 Markov Chain Analysis

At the receiver, a bit error would result in a chip error that not only will attenuate received signal strength at the output of the correlator, but will also propagate through the shift registers and affect the following bit decisions. The dynamic of the system performance during tracking can be investigated with Markov chain analysis.

For m chip errors, the amplitude attenuation at the correlator output is:

$$A|_m = \left|1 - \frac{2m}{N}\right| \qquad (3.4)$$

Thus, the conditional probability of error given m, $P_{e|m}$, is given as:

$$P_{e|m} = Q\left((1 - \frac{2m}{N})\sqrt{\frac{2E_b}{N_o}}\right) \qquad (3.5)$$

where $Q(.)$ is the Q-function and E_b / N_o is the symbol SNR under AWGN.

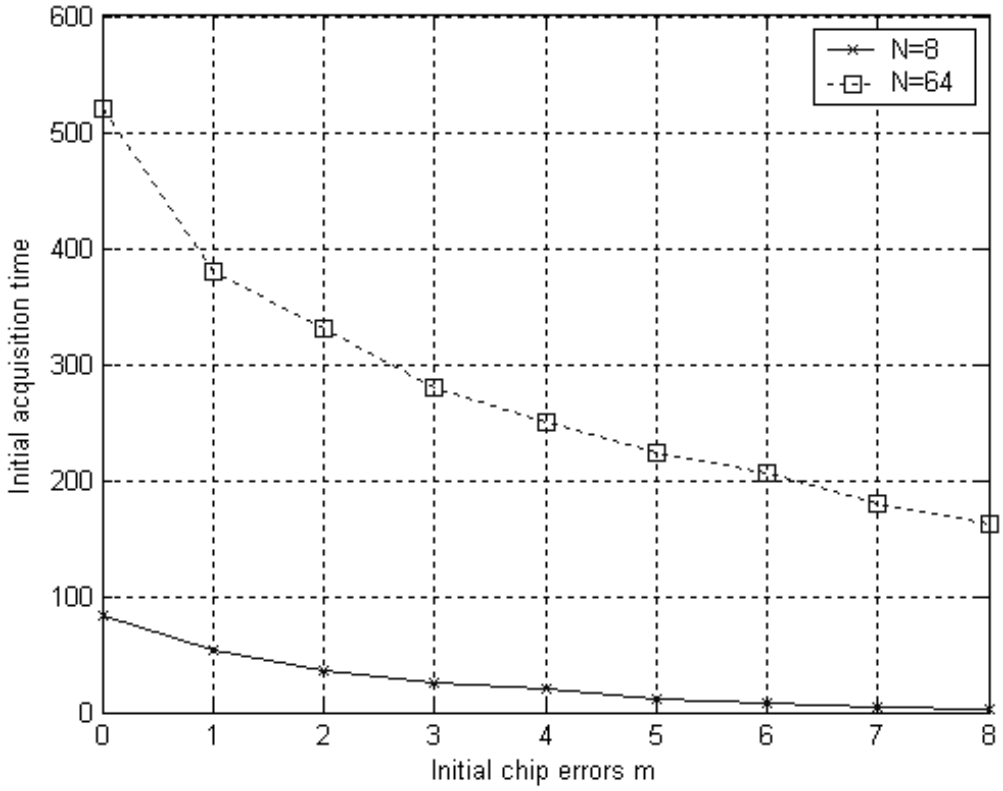

Fig. 3.3 Initial acquisition time $2L_1$ (bits) for $N = 8, 64$.

Let the state of the Markov chain be the error content of the receiver feedback shift register, with X_i representing the i-th state of the registers. For a spreading sequence of length N, there are 2^N states. Without loss of generality, we assume that N is even. The $2^N \times 2^N$ state transition matrix $\boldsymbol{P}$ of the Markov chain can be written as [20]:

$$\boldsymbol{P} = \begin{pmatrix} 1-P_{e|0} & P_{e|0} & 0 & 0 & & & & \\ 0 & 0 & 1-P_{e|1} & P_{e|1} & & & & \\ & & & & \dots & \dots & 0 & 0 \\ & & & & & & 1-P_{e|N-1} & P_{e|N-1} \\ 1-P_{e|1} & P_{e|1} & 0 & 0 & & & & \\ 0 & 0 & 1-P_{e|2} & P_{e|2} & & & & \\ & & & & \dots & \dots & 0 & 0 \\ & & & & & & 1-P_{e|N} & P_{e|N} \end{pmatrix} \tag{3.6}$$

This is an irreducible, positive-recurrent and aperiodic Markov matrix that describes an ergodic Markov chain, whose states are all positive-recurrent. The probability distribution of X_i converges to a steady state distribution as the number of the transmitted symbols increases.

The first entrance probability of a Markov chain is defined as:

$f_{ij}^{(n)} = Pr\{$starting from state i, the first passage to state j in exactly n steps$\}$

$$= \Pr\{X^n = X_j, X^{n-1} \neq X_j, \dots, X^1 \neq X_j \mid X^o = X_i\} \tag{3.7}$$

where X^n is the state at step n.

For the above ergodic Markov chain, the mean first passage time (MPT) from i chip

errors to j chip errors, denoted M_{ij} , is defined to be expected value of the number of steps n = 1,2,… Thus, M_{ij} can be computed as [20,36,37]:

$$M_{ij} = \sum_{n=1}^{\infty} n f_{ij}^{(n)} \tag{3.8}$$

Notice that for $i = j$, M_{ii} is called the mean recurrence time.

Let $\mathbf{M}$ be the matrix of the MPT. Then $\mathbf{M}$ can be computed iteratively, according to [20]:

$$\mathbf{M}^{(n+1)} = \mathbf{E} + \mathbf{P}[\mathbf{M}^{(n)} - diag(\mathbf{M}^{(n)})] \tag{3.9}$$

where $\mathbf{M}^{(0)} = \mathbf{E}$; $\mathbf{E} = ee^T$ with $e = (1,1,1,...,1)^T$ and $diag(.)$ is the matrix diagonal operation.

Equation (3.9) can be used to calculate the MPT once the transition matrix $\boldsymbol{P}$ is known. Table I shows the example MPT calculations for N = 8 with different SNR and initial chip errors m. The results show that MPT increases with SNR and m.

Table I. Mean First Passage Time for N = 8.

	SNR=3 dB	SNR=4 dB	SNR=5 dB	SNR=6 dB	SNR=7dB
M_{10}	29.765	32.602	35.23	35.863	34.5
M_{20}	84.628	131.77	223.5	397.68	748

M_{30}	189.01	380.01	859.9	2114.6	5747
M_{40}	334.65	771.95	2005.3	5687	18002

In the tracking phase, the content of the receiver registers transits from m initial errors to the error-free condition (m = 0). Thus, the average transmission length during tracking, L_2 (bits), is determined by the MPT of the Markov chain and corresponds to element M_{m0} in matrix **M**. The mean tracking time is then equal to L_2T_b.

The overall synchronization time, T_{syn}, is the summation of the mean initial acquisition time and tracking time:

$$T_{syn} = 2L_1T_b + L_2T_b = (2L_1 + L_2)T_b \qquad (3.10)$$

So the average number of transmitted bits during the synchronization process, i.e., from the initial random errors until the error-free state, is $L = 2L_1 + L_2$.

The genetic algorithm acquisition phase depends on the initial chip errors m: a larger value of m would lead to a faster acquisition time. However, during the tracking phase, the tracking time would increase as m increases. Thus, for the overall synchronization that considers both phases together, there is an optimum performance, i.e., fastest synchronization time from the initial random chip errors to zero chip error, which can be achieved with an optimum value of m.

3.3 Synchronization

Figure 3.4 compares the theoretical acquisition time $2L_1$ under large SNR, based on

equation (3), to the simulation results under increasing *SNR* (the GA pool consists of 100 sequences in the simulation). As would be expected, the results show that the acquisition time decreases as m increases. Also, as the *SNR* increases from 4dB to 8dB, the simulation results approach the theoretical calculation which represents a lower bound. The example plots for $N = 8$ demonstrate that the theoretical calculations of acquisition time agree very well with the simulation results under high *SNR*.

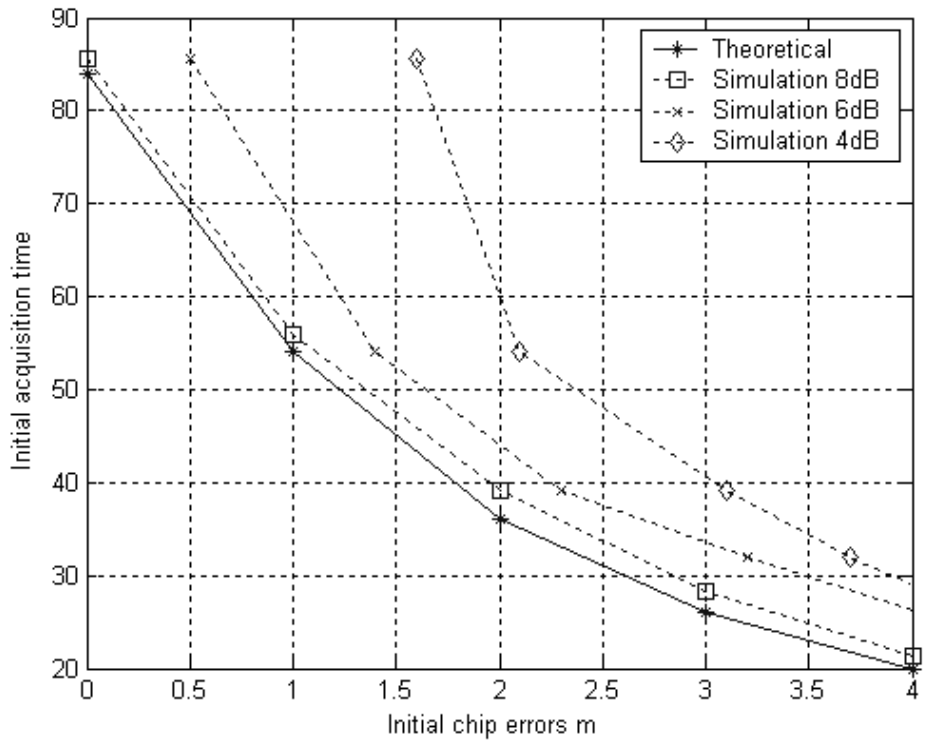

Fig. 3.4 Acquisition time $2L_1$ (bits) with SNR for $N = 8$.

Figures 3.5 and 3.6 plot the example tracking time for $N = 8$ based on Markov chain analysis and simulation, respectively, under increasing *SNR*. A direct comparison of the plots also demonstrates an excellent agreement between the analysis and the simulation. The results suggest that Markov chain analysis can accurately predict the mean tracking time.

Figure 3.7 compares theoretical calculation of the overall synchronization time, $2L_1+L_2$, to the simulation. The plots show that the theoretical and simulation results agree very well under high *SNR*. The plots in Fig. 3.7 demonstrate the validity of synchronization analysis by mean of genetic algorithm and Markov chain.

Figures 3.8 and 3.9 show the simulation results of initial acquisition time and tracking time, respectively, versus acquisition threshold for $N = 64$, as the *SNR* varies from 3dB to 8dB. Unlike the results in Fig. 3.4 for $N = 8$, the acquisition time for $N = 64$ in Fig. 3.8 does not change with the range of *SNR*. This suggests for a sufficiently large spreading length, the acquisition time is rather insensitive to *SNR*. On the other hand, the results in Fig. 3.9 show that the tracking time improves considerably with *SNR*.

Since the initial chip errors m decreases as the acquisition threshold increases, as expected the acquisition time $2L_1$ increases with the threshold as shown in Fig.3.8, while the tracking time L_2 decreases as the threshold increases as shown in Fig. 3.9.

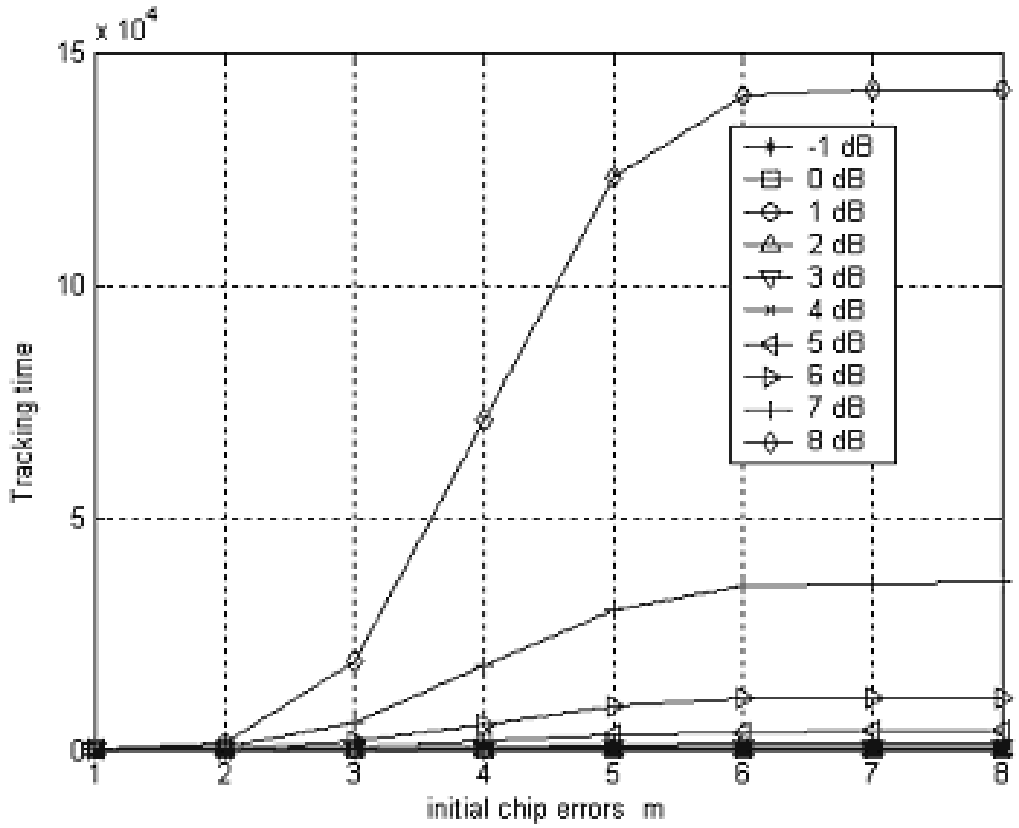

Fig. 3.5 Theoretical tracking time L_2 (bits) SNR for $N = 8$.

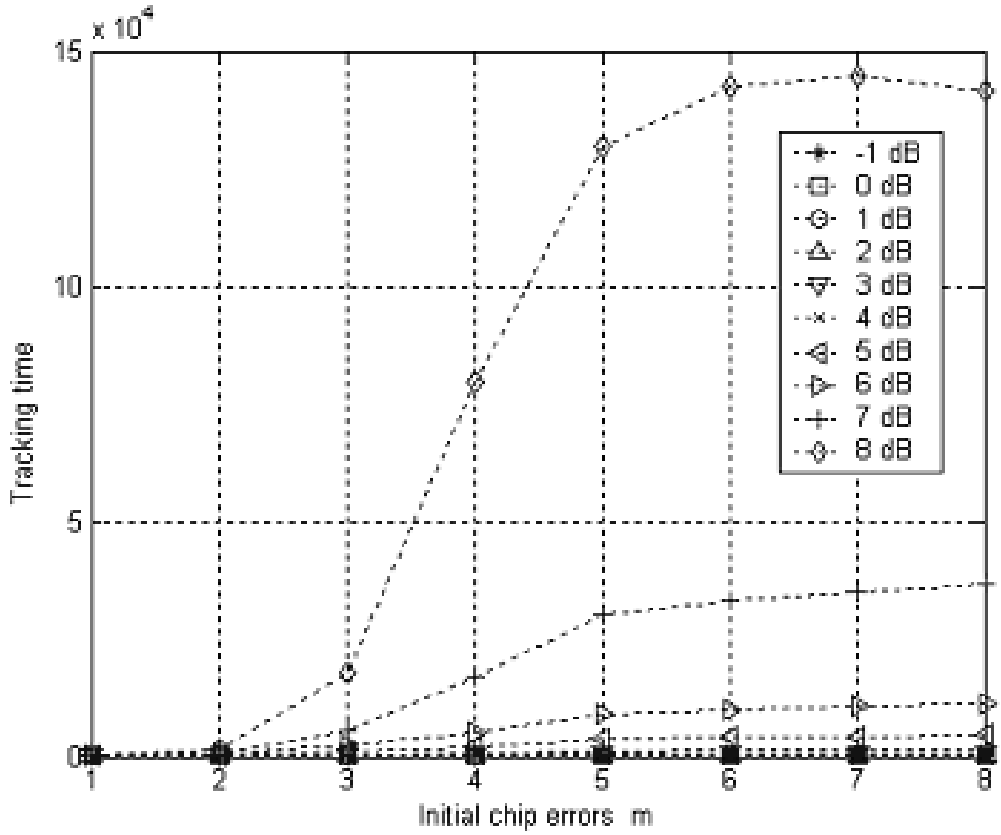

Fig. 3.6 Simulation of tracking time L_2 (bits) for $N = 8$.

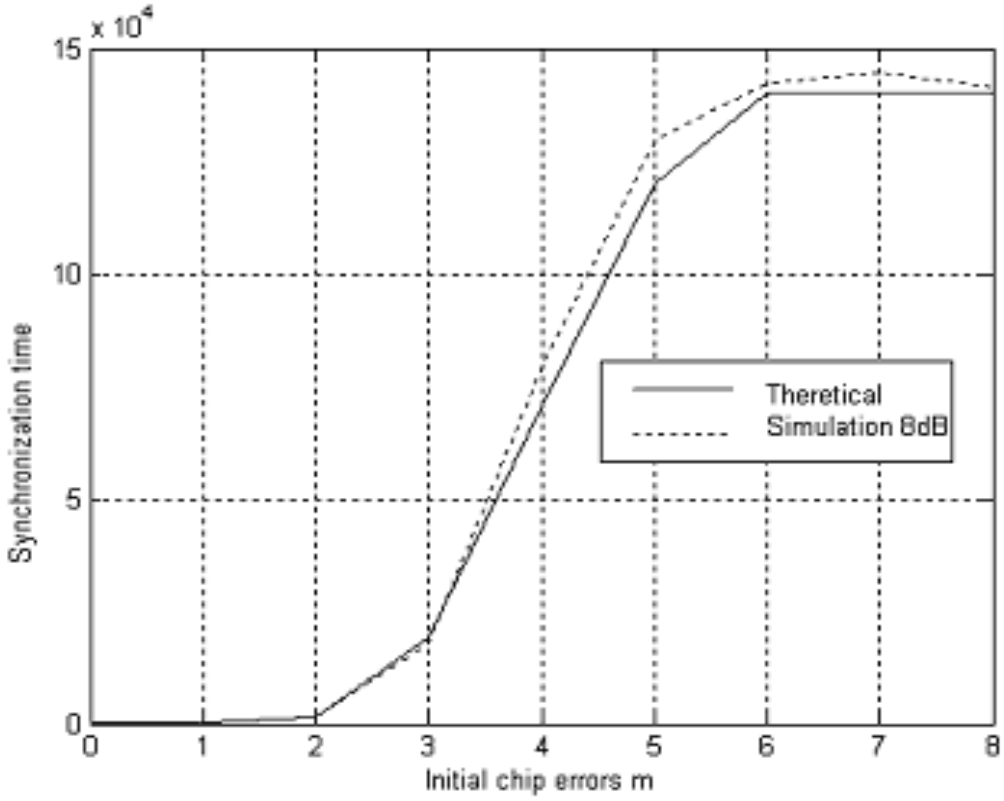

Fig. 3.7 Theoretical and simulation results of synchronization time, $2L_1 + L_2$ (bits), for $N = 8$ under high *SNR*.

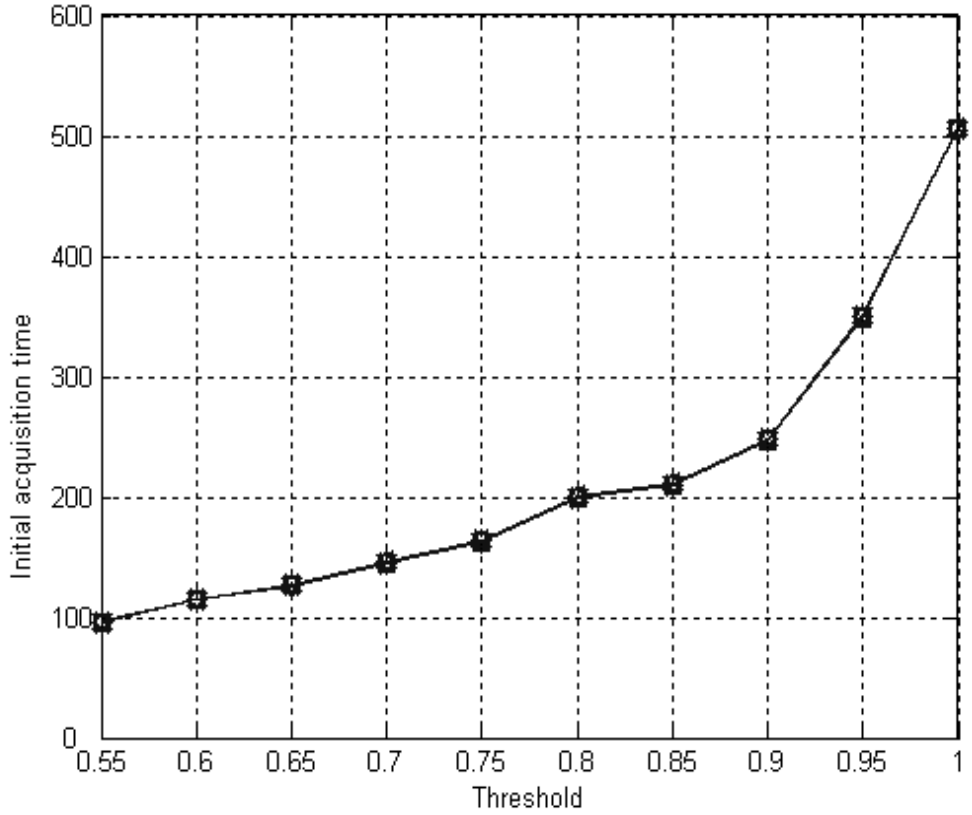

Fig. 3.8 Initial acquisition time $2L_1$ (bits) for $N = 64$.

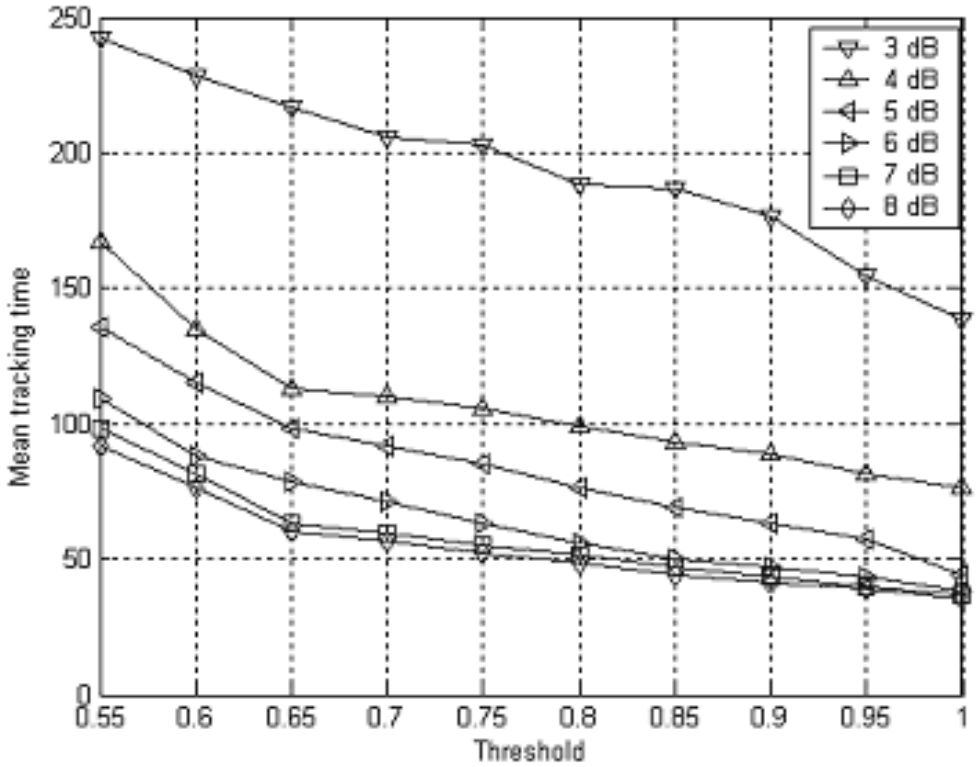

Fig. 3.9 Tracking time L_2 (bits) for $N = 64$.

Figure 3.10 plots the synchronization performance for $N = 64$ with the *SNR* varying from 3dB to 8dB. The plots show that the overall synchronization time, $L = 2L_1+L_2$, decreases as *SNR* increases. The results show that the synchronization process is clearly dominated by the initial acquisition phase ($2L_1$) when the correlation threshold is high (smaller m), while it is dominated by the tracking phase (L_2) when the threshold is low (larger m). Therefore, an optimum, fastest synchronization time can be achieved by setting an appropriate acquisition threshold.

As an example, Fig. 3.10 shows that for $N = 64$, an optimum threshold value of 0.65 would yield the minimum synchronization time of $L = 176$ bits at 8dB *SNR*.

The previous results have been obtained with a single correlator and a GA pool of 100 sequences. Intuitively, with additional (parallel) correlators and a larger sequence pool, the mean acquisition time would decrease and the minimum synchronization time therefore should improve [38].

Figure 3.11 shows that the example improvement in acquisition time (at 8dB *SNR)* is more significant for a larger threshold values as the number of correlators C increases from 1 to 32, with the sequence pool, S, fixed at 100. The acquisition time improvement with S increasing from 100 to 800, however, is marginal as shown in Fig. 3.12 for single correlator. Here we have fixed the good chromosome number with different pool size and mutation was not considered in the simulation. In Fig. 3.13, we use typical 90% cross-over and 5% mutation. The results show that:

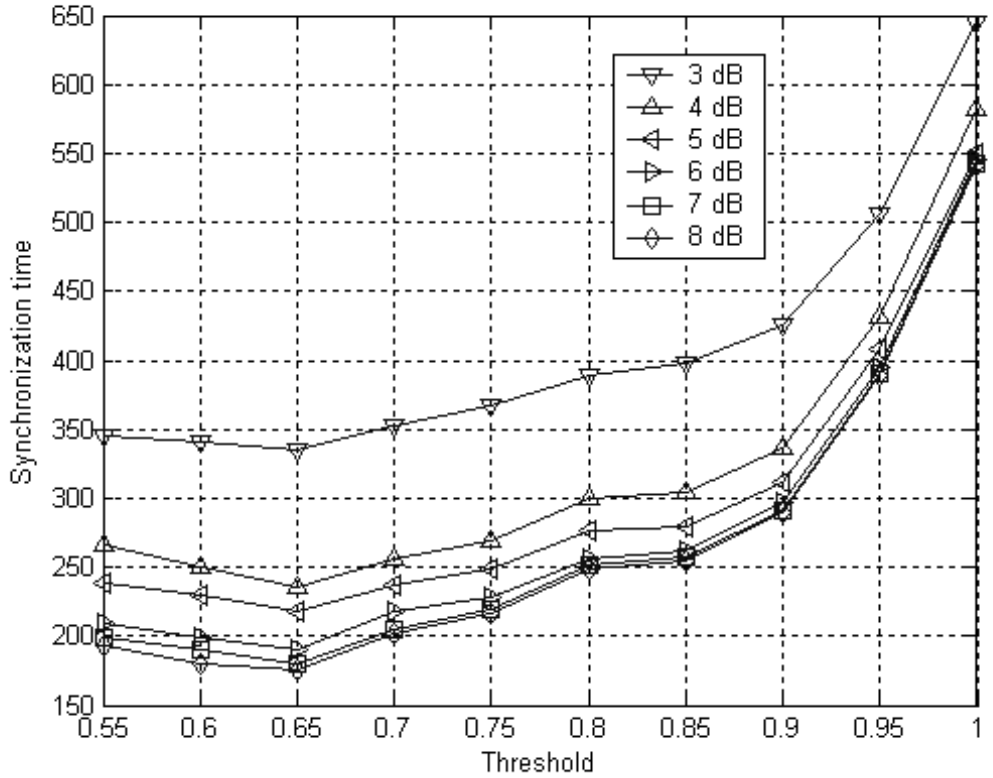

Fig. 3.10 Synchronization time $2L_1+L_2$ (bits) under different *SNR* for $N = 64$.

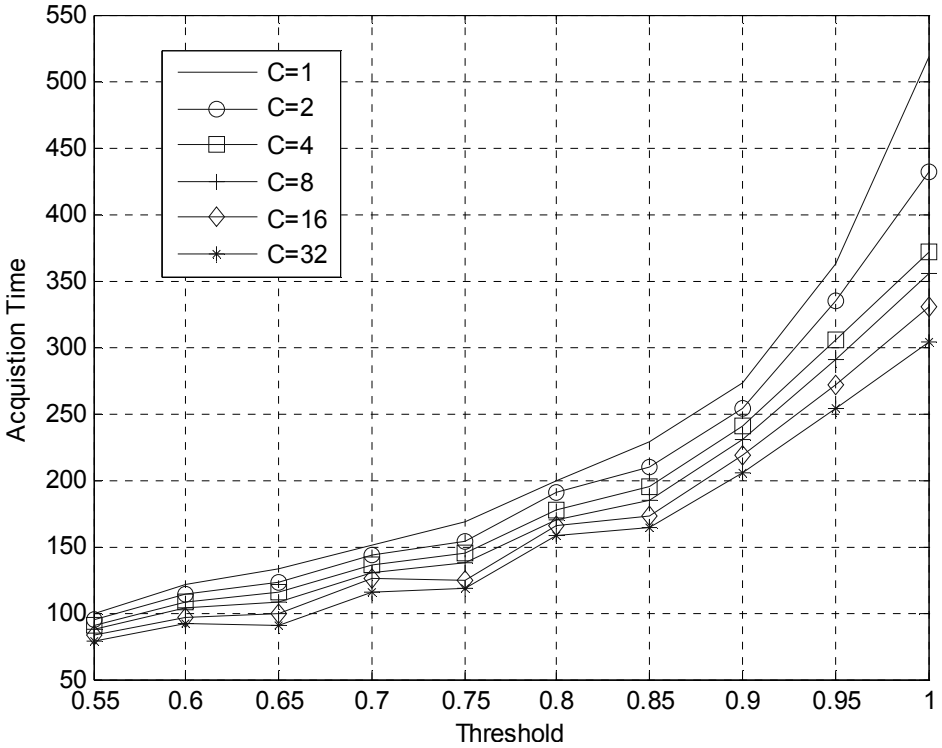

Fig. 3.11 Initial acquisition time $2L_1$ (bits) with parallel correlators for $N = 64$.

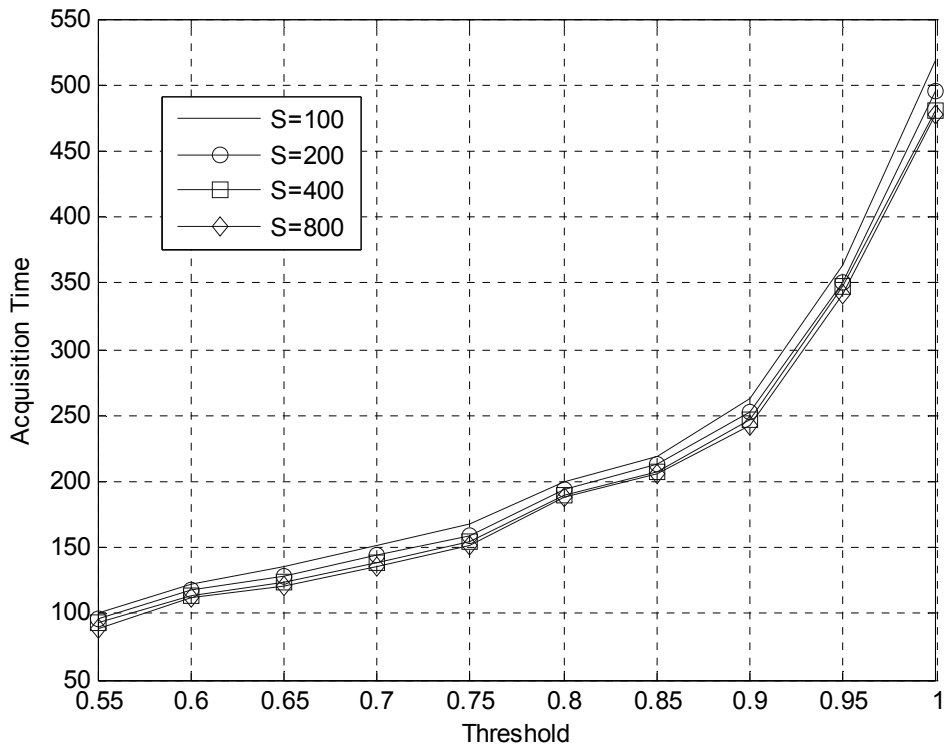

Fig. 3.12 Initial acquisition time $2L_1$ (bits) with larger sequence pool for $N = 64$.

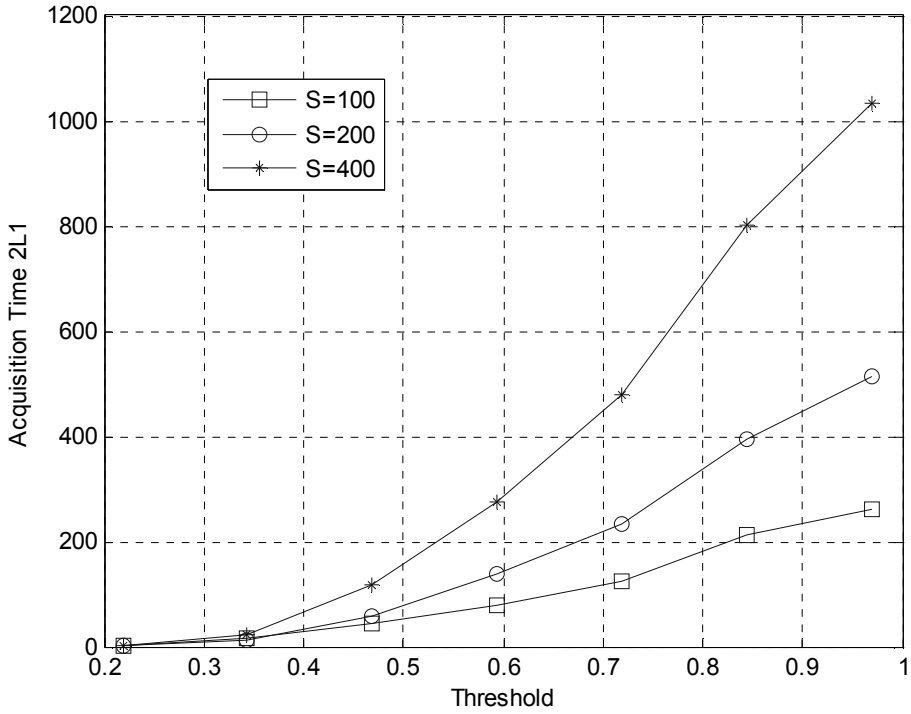

Fig. 3.13 Initial acquisition time $2L_1$ (bits) with larger sequence pools for cross-over=90% and mutation=5%

The smaller pool size of 100 is preferable.

Figure 3.14 demonstrates the overall synchronization performance improvement at 8dB *SNR* with additional correlators and a larger sequence pool. The example plots show that the minimum synchronization time has been reduced from 176 bits to 150 bits.

3.5 Summary

In this chapter, we considered SESS synchronization as the acquisition phase - from the initial random errors to m errors in the receiver registers, together with the tracking phase - from m errors to the error-free state. The mean initial acquisition time was computed by a genetic model and the mean tracking time was examined by Markov chain analysis. We explored the genetic model and Markov chain analysis theoretically and via simulation under different spreading length and *SNR* values. The results demonstrate the veracity of the theoretical modeling and analysis. We have shown that the acquisition time decreases as m increases, while the tracking time increases with m. Thus, for a given *SNR*, there is a minimum overall synchronization time that can be obtained by selecting an optimum acquisition threshold. The synchronization time can be improved further with parallel correlators and, to certain extend, a larger genetic sequence pool. The optimum SESS synchronization performance has been demonstrated with simulation results for an example spreading length of 64.

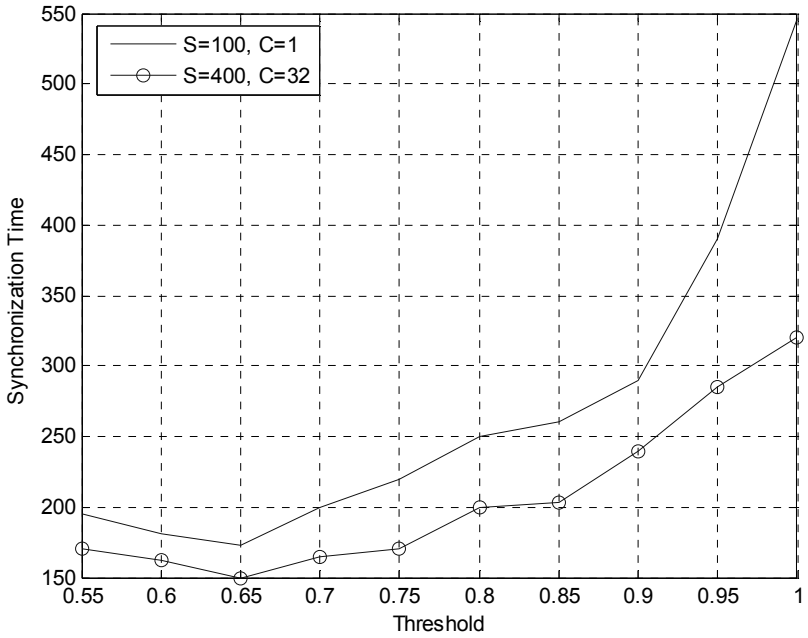

Fig. 3.14 Synchronization time $2L_1+L_2$ (bits) improvement with parallel correlators and a larger sequence pool for $N = 64$.

CHAPTER 4

Coded Cooperative Diversity with Spread Spectrum

4.1 Introduction

Multiple-input multiple-output (MIMO) techniques can be impractical in a wireless cellular system due to the small size and hardware complexity of the mobile terminals. Cooperative diversity (CD) has been proposed to overcome such limitation. In CD, several partner terminals around a given mobile terminal form a distributed cooperative network and transmit information collaboratively [21]. In this sense, CD offers similar advantages to existing diversity technique such as MIMO to combat the detrimental effects of multipath fading. CD technique is applicable for cellular, wireless LAN or ad-hoc network, where individual mobiles, PDAs or sensors communicate with a common base station or access point [21]. Sendonaris [6-7] has proposed a user cooperation model that achieved an increase in capacity. For further performance improvement, Laneman [25,39] has proposed a repetition-based and space-time-coded cooperation by mimicking MIMO system, but the repetition scheme reduces achievable rates. To avoid repeating symbols, Hunter has proposed a simple two users coded cooperation scheme [8]. The technology exploits the fact that around a given terminal, there can be other single-antenna terminals which can be used to enhance diversity by forming a distributed (or virtual) multi-antenna system. As demonstrated in [21] cooperative diversity can achieve a diversity order equal to the number of paths between

the source and the destination, and in this sense, they offer similar advantages to any existing diversity technique. Cooperative diversity has been attracting increasing attention as a novel and promising diversity technique.

In this chapter, we propose a cooperative convolutional coding (CCC) scheme with spread spectrum and present its performance in fading channels. CCC combines channel coding and cooperative diversity to simultaneously achieve both time diversity and space diversity, while maximum ratio combiner (MRC) only exploits space diversity gain [41]. The coded bits are spread using orthogonal spreading sequences. The spread code bits are added and transmitted simultaneously. We also applies the power scaling factor to the transmit signal to maintain the same average power and show that CCC outperforms MRC without an average power increase. We compare simulation result to the repetition scheme with MRC and show how bit-loss in hostile channels influences the performance of CCC.

4.2 Coded Cooperative Diversity System Model

User cooperative diversity was introduced as a way to obtain multiple antenna gains even when each user has only one antenna. It is applicable to sensor or mobile communication networks, where, individual sensors, mobiles, or PDAs communicate with a common base station (BS) or access point (AP).

Figure 4.1 shows the block diagram of the cooperative network where information is communicated between a source (S=R_1) and a destination (D=R_0) over a complex channel

with fading parameter f_{10}. Two relay nodes, R_2 and R_3 , are willing to cooperate to provide repeated signals through the complex channels with flat fading channel parameters (f_{12}, f_{13}) from (S) to (R_2, R_3), and (f_{20}, f_{30}) from (R_2, R_3) to (D), respectively. Without loss of generality, we assume the relays and destination have the same additive white Gaussian noise (AWGN) power. We also assume that the values of random variables, f_{10}, f_{12}, f_{13}, f_{20} and f_{30} have been determined at the receiver ends by training. We consider the Amplify and Forward (AF) model with a constant average power.

The basic idea in our proposed CCC is to implement convolutional coding across a cooperative relay network, as shown in Figure 4.2. In this chapter, to exploit time diversity for the CCC system against fading, we employ an example convolutional code with a constraint length (K) of 3, a code rate (R) of 1/3, and the corresponding free distance (d_{free}) equals to 6 [40,54]. The code generator is (5,7,4) in octal representation [24,60]. Let the convolutional code sequence be: $d_1 \oplus d_3$, $d_1 \oplus d_2 \oplus d_3$ and d_3 where $\oplus$ denotes the exclusive OR operation. The three code words will be orthogonally spread, added and transmitted through the direct and relay paths simultaneously with different channel fading coefficients.

The receiver despreads the three convolutional code bits and combines using MRC scheme, followed by Viterbi decoding with soft decision [42-43]. The receiver thus exploits the additional time diversity as well as the spatial diversity inherent in relay systems.

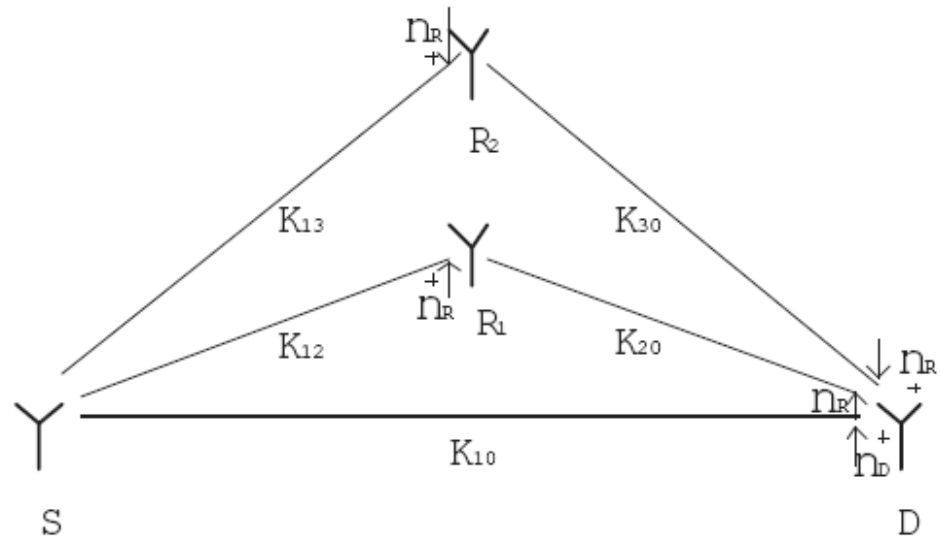

Fig. 4.1. Cooperative Diversity structure.

4.3 Coded Cooperative Diversity System Analysis

4.3.1 BER for Relay Channel (MRC)

Let the mean and the second moment (power) of the fading coefficents, f_{ij} are equal to K_{ij} and ξ_{ij}, respectively. As shown in Fig. 4.1, $K_{10}\, K_{12}\, K_{13}\, K_{20}$ and K_{30} are the mean of the fading coefficients on the relay paths, and so the instantaneous signal-to-noise ratio (SNR) at the different branches can be calculated as:

$$\gamma_{ij} = \xi_{ij} \frac{P_x}{N_o} \qquad (i = 1,2,3 \quad j = 0,2,3) \tag{4.1}$$

The instantaneous SNR at receiver with diversity can be derived as [21]:

$$\gamma_z = \sum_{k=2}^{3} \frac{\gamma_{1k}\gamma_{k0}}{1 + \gamma_{1k} + \gamma_{k0}} + \gamma_{10} \cdot \tag{4.2}$$

At high *SNR*, (4.2) simplifies to

$$\begin{aligned} \gamma_z &= \sum_{k=2}^{3} \frac{\gamma_{1k}\gamma_{k0}}{\gamma_{1k} + \gamma_{k0}} + \gamma_{10} \\ &= \sum_{k=2}^{3} \frac{1}{\frac{1}{\gamma_{1k}} + \frac{1}{\gamma_{k0}}} + \gamma_{10} \cdot \end{aligned} \tag{4.3}$$

In MRC cooperative scheme, information bits are repeated in relay paths. We assume binary phase-shift keying modulation (BPSK) over Rayleigh fading channels. Therefore, the bit error rate is:

$$P_e = \binom{2M+1}{M+1} \cdot 4^{-(M+1)} \cdot \frac{1}{\gamma_{10}} \cdot \prod_{k=2}^{3} \left(\frac{1}{\gamma_{1k}} + \frac{1}{\gamma_{k0}}\right) \tag{4.4}$$

Here, the relay nodes number M=2, then

$$P_e = \frac{5}{32} \left(\frac{1}{E_b / N_o}\right)^3 \left(\frac{1}{\xi_{12}} + \frac{1}{\xi_{20}}\right)\left(\frac{1}{\xi_{13}} + \frac{1}{\xi_{30}}\right)\frac{1}{\xi_{10}} \tag{4.5}$$

The error probability P_e is the function of $(E_b / N_o)^{-(M+1)}$ [8]. Therefore, the cooperative

network can achieve the full diversity order $M+1$.

4.3.2 BER for Cooperative Convolutional Coding (CCC)

In CCC cooperative scheme, three code words will be spread with orthogonal sequences and added. After applying the power scaling factor, the signal is transmitted through the direct path and relay paths simultaneously as shown in Figure 4.2.

The transmitted signal x can be expressed as:

$$x = C\{(d_1 \oplus d_3)S_1 + (d_1 \oplus d_2 \oplus d_3)S_2 + d_3 S_3\} \tag{4.6}$$

where S_1, S_2, S_3 are orthogonal spreading sequences and C is the power scaling factor.

The received signals can be expressed as:

$$y_1 = f_{10}x + n_1$$

$$y_2 = f_{12}A_2 f_{20}x + n_2$$

$$y_3 = f_{13}A_3 f_{30}x + n_3 \tag{4.7}$$

where A_2 and A_3 are amplification factors to maintain constant average power output of the relays:

$$A_2 = \sqrt{(E_b/N_o)/(f_{12}^2(E_b/N_o)+1)}$$

$$A_3 = \sqrt{(E_b/N_o)/(f_{13}^2(E_b/N_o)+1)} \tag{4.8}$$

n_1, n_2, n_3 are statistically independent and Gaussian distributed as $N(0,\sigma_0^2)$. We obtain the code words for Viterbi decoding as follows:

$$C_1 = \psi_1 y_1 S_1 + \psi_2 y_2 S_1 + \psi_3 y_3 S_1$$

$$C_2 = \psi_1 y_1 S_2 + \psi_2 y_2 S_2 + \psi_3 y_3 S_2$$

$$C_3 = \psi_1 y_1 S_3 + \psi_2 y_2 S_3 + \psi y_3 S_3 \tag{4.9}$$

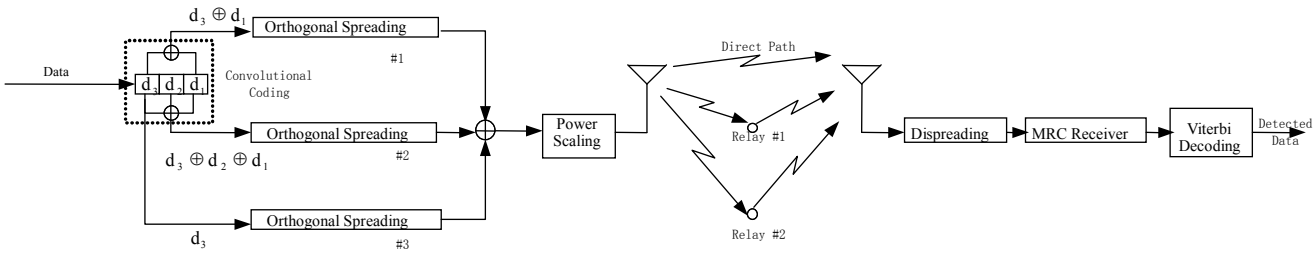

Fig. 4.2 Cooperative diversity structure with convolutional coding.

Here ψ_1, ψ_2 and ψ_3 are the normalization factors for fading, relay and destination noise power. The normalization factors are obtained as:

$$\psi_1 = f_{10} / \sigma_0^2$$
$$\psi_2 = f_{20} A_2 f_{12} /((f_{20}^2 A_2^2 + 1)\sigma_0^2)$$
$$\psi_3 = f_{30} A_3 f_{13} /((f_{30}^2 A_3^2 + 1)\sigma_0^2) \quad (4.10)$$

We assumed the same noise power σ_0^2 at relays and the destination.

4.4 Simulation results

We simulate cooperative performance of CCC and MRC with BPSK modulation in Rayleigh fading channels. The relay nodes number *M*=2, or three branches.

Figure 4.3 presents the BER of CCC with a soft-decision Viterbi decoding in independent channels. The BER of MRC is also plotted for comparison [21]. In Figure. 4.3, we assumed the expected fading coefficients are identical for the relay channels. The simulation result shows that CCC improves the system performance significantly over MRC-based cooperative systems.

In the following, we specifically simulate MRC and CCC schemes with the following two groups of fading coefficients:

Case 1:

$K_{10} = K_{20} = K_{30} = 0.5$, $K_{12} = K_{13} = 0.5$

Case 2:

$K_{10} = K_{20} = K_{30} = 0.2$, $K_{12} = K_{13} = 0.9$

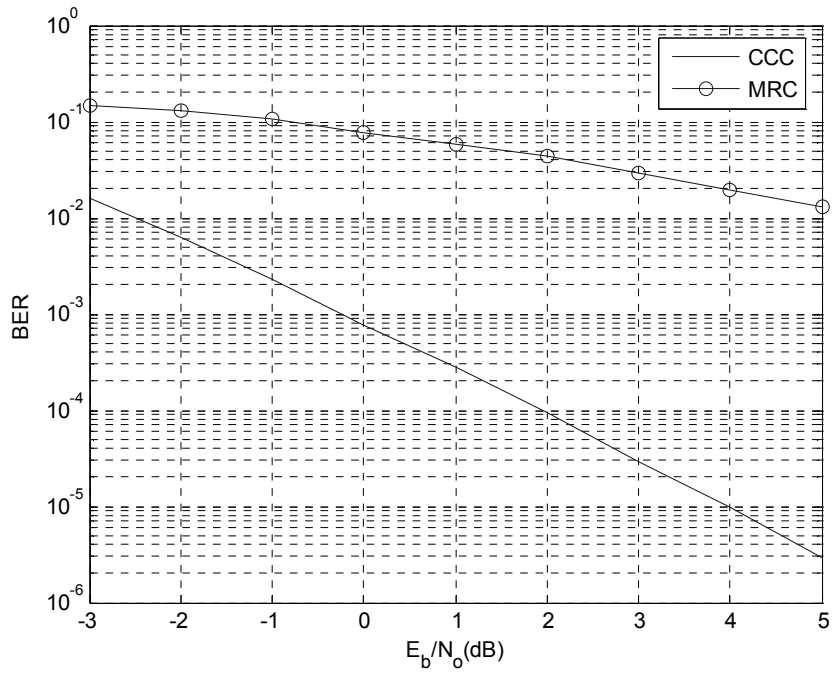

Fig. 4.3 Simulation BER, CCC and MRC, $K_{10}=K_{20}=K_{30}=1$, $K_{12}=K_{13}=1$.

The relays in Case 1 are between the source and destination. Figure 4.4 shows the analytical and simulation BER of MRC for both cases. The analytical BER based on equation (4.5) agree well with the simulation results under high SNR as expected. The results show that having the relays between the source and the destination exhibits a better performance as estimated in [21]. We have also obtained similar results for Case 2 with a slightly degraded performance.

Figures 4.5 and 4.6 plot the BER of MRC and CCC in correlated channels. The performance degrades as the correlation value increases. We observed a similar degradation with CCC as shown in Figure 4.6. Notice that the BER performance degrades greatly if channels are fully correlated (R=1) in both schemes.

Figures 4.7 and 4.8 show the BER of MRC and CCC when the bits are lost, for example, in hostile channels. The results show that with CCC, the BER degradation is more gradual than MRC. The time diversity achieved by convolutional coding and the soft-decision Viterbi decoding in CCC allows the receiver to mitigate system degradation due to the bit loss.

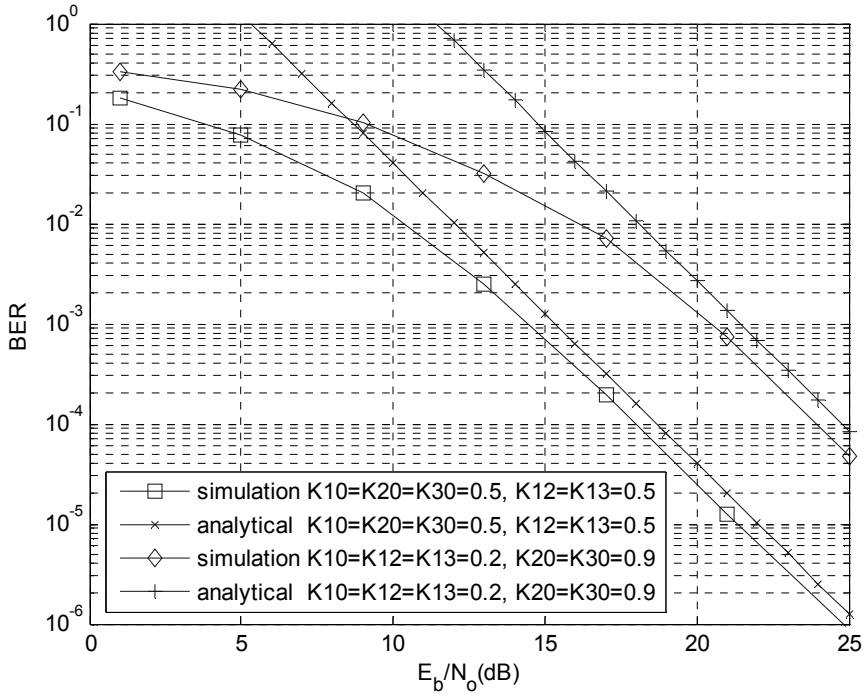

Fig. 4.4 Analytical and simulation BER of MRC.

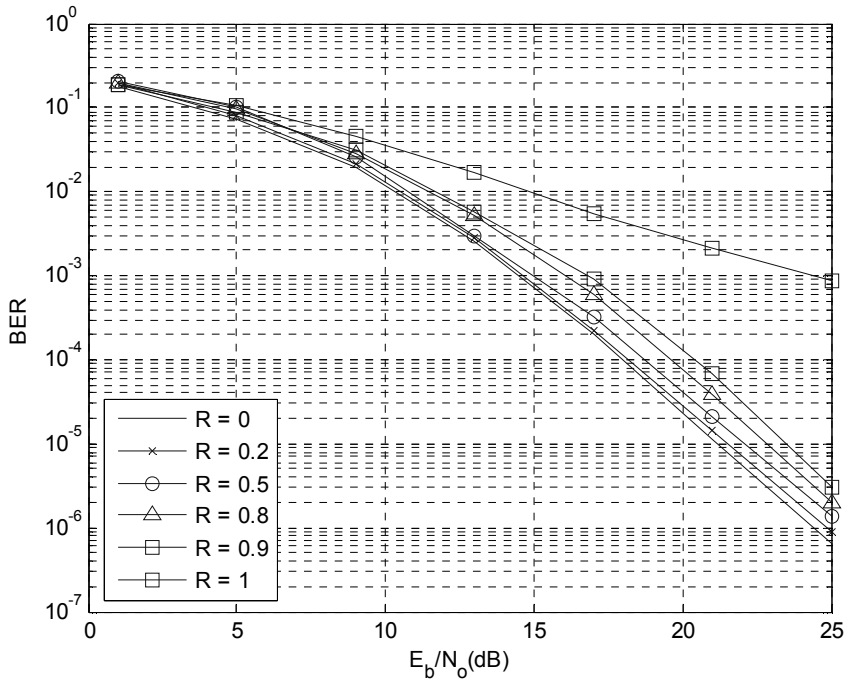

Fig. 4.5 Simulation BER of MRC with $K_{10} = K_{20} = K_{30} = 0.5$, $K_{12} = K_{13} = 0.5$, for various correlation values of correlated channel.

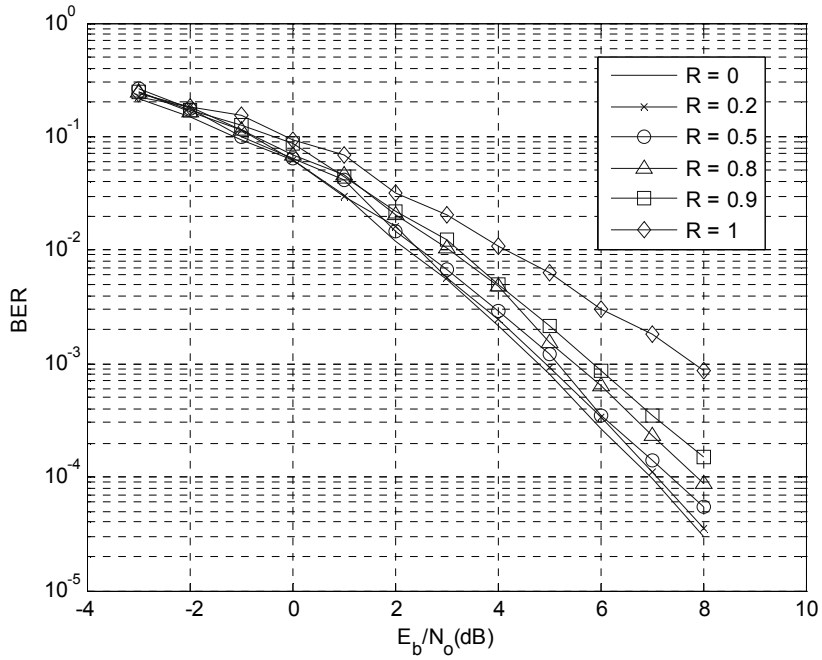

Fig. 4.6 Simulation BER of CCC with $K_{10}=K_{20}=K_{30}=0.5$, $K_{12}=K_{13}=0.5$, in correlated channel.

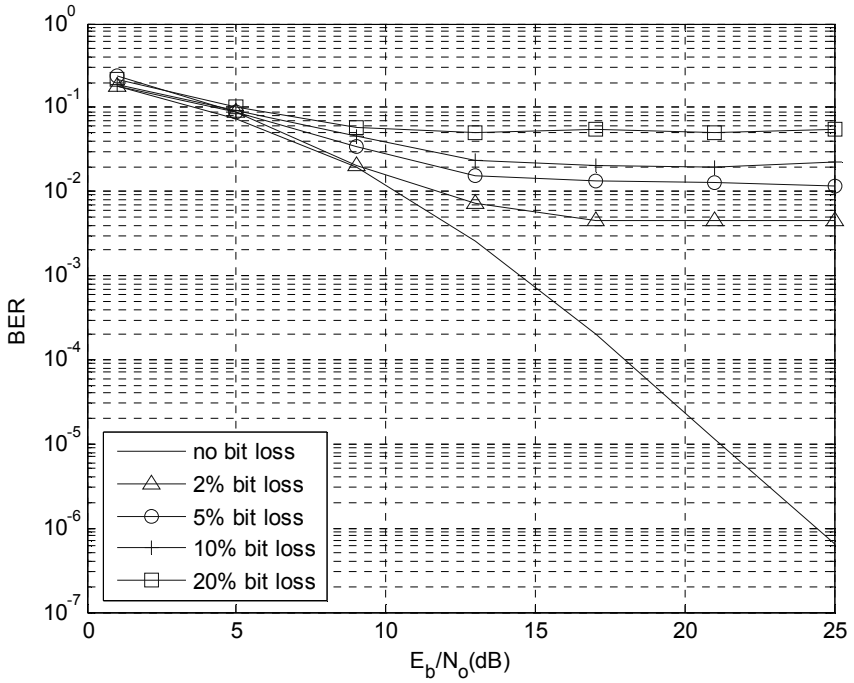

Fig. 4.7 Simulation BER of MRC with $K_{10} = K_{20} = K_{30} = 0.5$, $K_{12} = K_{13} = 0.5$, for various bit loss percentages.

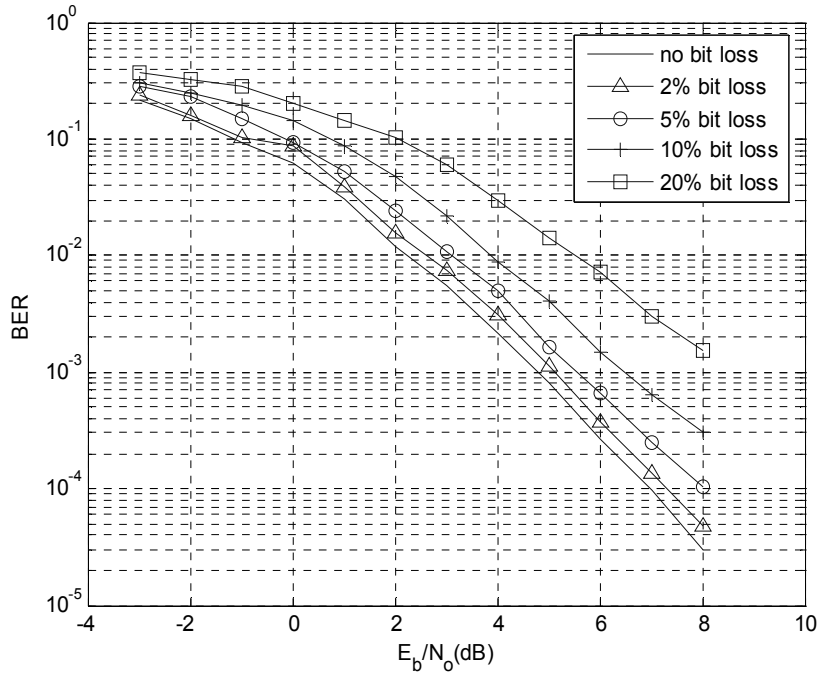

Fig. 4.8 Simulation BER of CCC with $K_{10}=K_{20}=K_{30}=0.5$, $K_{12}=K_{13}=0.5$, for various bit loss percentages.

4.5. Summary

In this chapter, we proposed a CCC cooperative scheme that simultaneously exploits time diversity as well as spatial diversity without an average power increase. We presented the performance of CD links with convolutional coding and spread spectrum. The relays amplify and forward their received signals from the source to the destination. Using Viterbi decoding with soft decision, the proposed CCC scheme achieves diversity gain with the number of cooperating relays in correlated channels and under bit loss environments. CCC imposes additional burden of encoding and decoding complexity in the mobile and base stations, respectively. The simulation results show that the proposed CCC exhibits significant gain over MRC relay systems.

CHAPTER 5
Self-encoded Spread Spectrum with Cooperative Diversity

5.1 Introduction

This chapter analyzes the cooperative SESS for Amplify and Forward CD links in rayleigh channels. The results show that our cooperative SESS improves the system performance significantly over MRC-based cooperative systems.

In section 5.2, we describe the system model. Section 5.3 analyzes the performance of Cooperative SESS and MRC. The analytical and simulation results based on cooperative convolutional coding schemes are presented in section 5.4. The conclusion follows in section 5.5.

5.2 Cooperative SESS System Model

The basic idea in our proposed spatially cooperative spread spectrum is to implement SESS across a cooperative relay network. At the transmitter, the delay registers are constantly updated from N-tap serial delay of the data to generate the spreading sequence of length N. The current bit is spread by the time varying N chip sequence that has been obtained from the previous N data bits [22].

The SESS data bit will be transmitted through the direct and relay paths

simultaneously with different fading coefficients as shown in Fig. 5.1. The self-encoding operation at the transmitter is reversed at the receiver. The recovered data are fed back to the *N*-tap delay registers that provide an estimate of the transmitter spreading code required for signal de-spreading [44]. The SESS-CD receiver employs iterative detection.

The receiver thus exploits the additional time diversity as well as the spatial diversity inherent in relay systems. The transmitted signal can be expressed as:

$$x = d_i S_i \tag{5.1}$$

where d_i and S_i are the data bit and the SESS spreading sequence, respectively, during i-th bit duration. Then, the output of the decorrelator at the receiver is given by

$$r_i = \psi_1 y_1 S_i^* + \psi_2 y_2 S_i^* + \psi_3 y_3 S_i^* \tag{5.2}$$

where S_i^* is the recovered spreading sequences at the receiver, which may be different from S_i due to the detection errors. y_1, y_2, y_3 are received signals as in (4.7) ψ_1, ψ_2 and ψ_3 are the normalization factors for fading and noise power:

$$\begin{aligned} \psi_1 &= f_{10} / \sigma_0^2 \\ \psi_2 &= f_{20} A_2 f_{12} /((f_{20}^2 A_2^2 + 1)\sigma_0^2) \\ \psi_3 &= f_{30} A_3 f_{13} /((f_{30}^2 A_3^2 + 1)\sigma_0^2) \end{aligned} \tag{5.3}$$

We can write SESS signals as

$$\mathbf{S} = \underbrace{\begin{bmatrix} S_1 = & d_0 & d_{-1} & d_{-2} & \dots & d_{-N+1} \\ S_2 = & d_1 & d_0 & d_{-1} & \dots & d_{-N+2} \\ S_3 = & d_2 & d_1 & d_0 & \dots & d_{-N+3} \\ & \vdots & \vdots & \vdots & \vdots & \vdots \\ S_N = & d_{N-1} & d_{N-2} & d_{N-3} & \dots & d_0 \\ S_{N+1} = & d_N & d_{N-1} & d_{N-2} & \dots & d_1 \end{bmatrix}_{[(N+1)\times N]}}_{\text{spread sequence block}} \tag{5.4}$$

where d_i are the data bits delayed to form the SESS spreading sequences. Since the current bit is spread by N previous bits, we can observe that current detecting bit d_1 is also related to previous N information bits, which are stored in the delay shift register $d_{-N+1\dots}$ d_0. By incorporating previous detected bits, we expect to improve the performance [45]. Therefore signal energy can be retrieved from previous estimated bits as:

$$\xi_i = \sum_{i=1}^{N} r_{k-i} c_{k-i} \tag{5.5}$$

and, the bit decision can be made based on

$$Y_i = r_i + \xi_i \tag{5.6}$$

For MRC scheme, we obtain

$$Y_i = \psi_1 y_1 + \psi_2 y_2 + \psi_3 y_3 \tag{5.7}$$

at the receiver for bit detection. We assume that each relay path and direct path is isolated. The isolation can be achieved by time division multiplexing.

5.3 Cooperative SESS System Analysis

a) BER for Relay Channel (MRC): As shown in Fig 5.1, f_{10}, f_{12}, f_{13}, f_{20} and f_{30} are the

fadings on the relay and direct paths. With the mean and the second moment (power) of the fading, f_{ij} are equal to K_{ij} and ξ_{ij}, respectively, the signal-to-noise ratio (SNR) at different nodes can be calculated as:

$$\gamma_{ij} = \xi_{ij} \frac{P_x}{N_o} \tag{5.8}$$

where Px / No is the received SNR in AWGN channels without fading. The SNR at receiver with diversity can be derived from [21] as

$$\gamma_z = \sum_{k=2}^{3} \frac{\gamma_{1k}\gamma_{k0}}{1+\gamma_{1k}+\gamma_{k0}} + \gamma_{10} \tag{5.9}$$

which is reduced to

$$\gamma_z = \sum_{k=2}^{3} \frac{\gamma_{1k}\gamma_{k0}}{1+\gamma_{1k}+\gamma_{k0}} + \gamma_{10} = \sum_{k=2}^{3} \frac{1}{\frac{1}{\gamma_{1k}}+\frac{1}{\gamma_{k0}}} + \gamma_{10} \tag{5.10}$$

At high SNR. In MRC cooperative scheme, information bits are repeated in relay paths. We assume binary phase-shift keying modulation (BPSK) over Rayleigh fading channels. Therefore, the bit error rate with M relay branches is [21]:

$$P_e \approx \frac{C(M)(K+1)^{M+1}}{k^{M+1}} \frac{1}{\gamma_{10}} \prod_{m=1}^{M} \left(\frac{1}{\gamma_{1m}} + \frac{1}{\gamma_{m0}}\right) \tag{5.11}$$

where K denotes the specular factor in non-central Chi-squared distribution, and $K = 0$ for exponential distribution. The constant k depends on the type of modulation, and $k = 2$ for binary phase shift keying [46]. $C(M)$ can be obtained as

$$C(M) = \frac{\prod_{k=1}^{M+1}(2k-1)}{2(M+1)!} \tag{5.12}$$

If the relay nodes number M=2, then

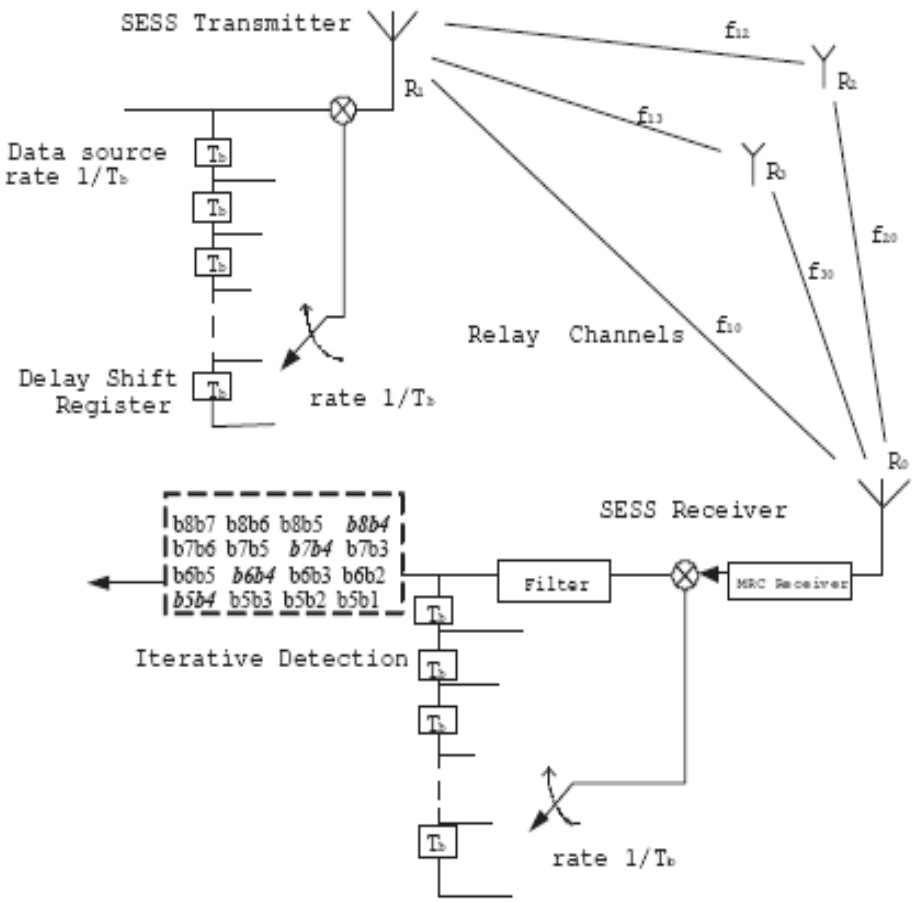

Fig. 5.1. Cooperative Self-encoded Spread Spectrum structure.

$$P_e = \frac{5}{32}\left(\frac{1}{E_b / N_o}\right)^3\left(\frac{1}{\xi_{12}} + \frac{1}{\xi_{20}}\right)\left(\frac{1}{\xi_{13}} + \frac{1}{\xi_{30}}\right)\frac{1}{\xi_{10}} \qquad (5.13)$$

We observe that the error probability P_e is the function of $(E_b/N_o)^{-(M+1)}$ where M is the number of relay nodes. Therefore, the cooperative network can achieve the full diversity order of M+1 [47].

b) BER for Self-encoded Spread Spectrum Cooperative Diversity (SESS-CD): The performance of SESS-CD with iterative detection can be considered as

$$P_e = \int_0^\infty Q(\sqrt{k\gamma_z})p_{\gamma_z}(\gamma_z)d\gamma_z \qquad (5.14)$$

where $p_{\gamma_z}(\gamma_z)$ is the probability density function of γ_z. In this cooperative SESS-CD performance analysis, we do not consider the self-interference that comes from the erroneous dispreading sequences due to the incorrect bit decision at the receiver. (self-interference has been shown to be dominant only at low SNR or with small spreading factors [26]). The received energy in each path can be considered as

$$y = \alpha_0 + \sum_{i=1}^{N}\alpha_i, \qquad (5.15)$$

where α_i for i = 1,…,N is an exponential random variable (r.v) with parameter $1/\gamma_c$, i.e.,

$$p_{\alpha_i}(\gamma) = \frac{1}{\gamma_c}\exp\{\gamma/\gamma_c\} \qquad (5.16)$$

where γ_c is the chip energy-to-noise ratio with fading, and α_0 is an exponential r.v. with parameter $N\gamma_c$. The first term in Eq. (5.15) is the output of the current despreading bit and the second term is the iterative detection output. We apply the central limit theorem to find the approximate probability density function (pdf) of y as

follows. Since the mean and variance of α_i, for $i > 1$ are γ_c and γ_c^2, respectively, we can approximate the mean and variance of y in Eq. (5.15) as:

$$m_y = N\gamma_c + N\gamma_c = 2N\gamma_c \tag{5.17}$$

$$\sigma_y^2 = N^2\gamma_c^2 + N\gamma_c^2 = N(N+1)\gamma_c^2 \tag{5.18}$$

Therefore, the Gaussian pdf approximation pdf of y is

$$p_y(y) = \frac{1}{\sqrt{2\pi\sigma_y^2}} \exp\{-(y-m_y)^2/(2\sigma_y^2)\} \tag{5.19}$$

Since the first term in Eq. (5.15) is a dominant term, Eq. (5.19) may not be the best approximation. However, we will find that the result can provide a useful insight regarding the SESS-CD diversity gain. For high SNR, $p_y(0)$ tends to be zero. Therefore, we will find the $\partial p(0)/\partial y$ to be applied to the initial value theorem of Laplace Transforms [21] as

$$\frac{\partial p(0)}{\partial y} = \frac{1}{\sqrt{2\pi\sigma_y^2}} \exp\{\ m_y{}^2/2\sigma_y^2\} \tag{5.20}$$

$$\approx \sqrt{\frac{2}{\pi}} \exp\{-2\} \frac{1}{N^2} \frac{1}{\gamma_c^2} = \sqrt{\frac{2}{\pi}} \exp\{-2\} \frac{1}{\gamma_b^2}, \quad \text{for large } N \tag{5.21}$$

where γ_b is the bit energy to noise ratio with fading. The SNR at different nodes can be represented as γ_{ij}. With M cooperating branches, the probability of bit error with BPSK can be obtained as

$$P_e \approx \frac{C(M)(K+1)^{2(M+1)}}{k^{2(M+1)} a^{M+1}} \frac{1}{\gamma_{10}^2} \prod_{i=1}^{M} \left(\frac{1}{r_{1i}^2} + \frac{1}{r_{i0}^2}\right), \tag{5.22}$$

where $a = (\sqrt{2/\pi}\exp(-2))^{-1}$ from Eq. (5.22). $C(M)$ can be obtained as

$$C(M) = \frac{\prod_{k=1}^{2(M+1)} (2k-1)}{2(2(M-1))!} \tag{5.23}$$

Comparing Eqs. (5.11) and (5.22), we find that the effective SNR in SESS-CD with iterative detection is the square of the actual SNR.

5.4 Simulation Result

In Fig. 5.2, we can see that the performance of SESS-CD is superior to MRC. The result can be predicted from Eqs. (5.11) and (5.22). The BER difference between SESS-CD simulation and analysis comes from the Gaussian approximation of the received signal power. The exact pdf and its Gaussian approximation of the received signal power over random fading channels are shown in Fig. 5.3. We can observe that the Gaussian approximation shifts the distribution toward higher received signal power at both Eb/No equal to 5 dB and 10 dB, while maintaining the same mean and variance as the exact pdf. However the slope of SESS-CD simulation BER and analytical BER agrees well. The diversity gain determines the slope of the BER versus average SNR curve, at high SNR, in a log-log scale. On the other hand, coding gain (in decibels) determines the shift of BER curve in SNR relative to the benchmark curve in uncoded communication over a random fading channel [23]. We see that the Gaussian approximation exhibits a rather accurate diversity gain but not coding gain. The diversity gain in Fig. 5.2 portrays well the square term of the SNR enhancement in SESS-CD in Eq. (5.22). Fig. 5.4 shows the performance of SESS-CD with different relay locations. The relay location

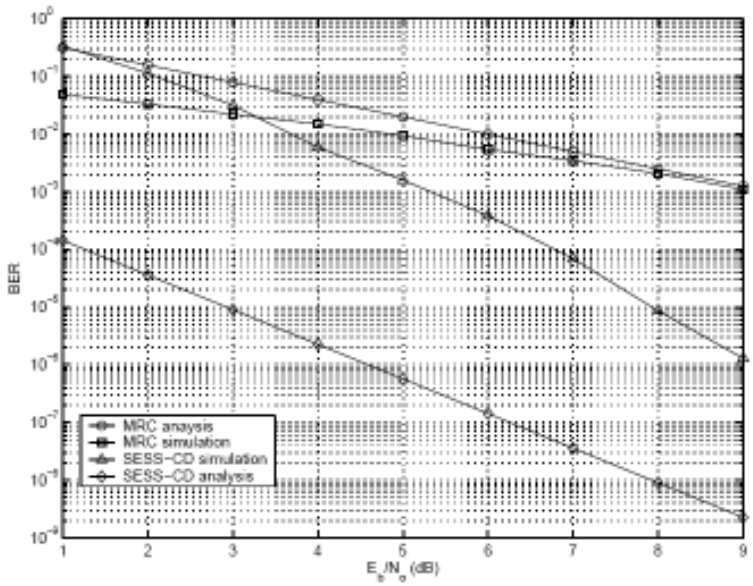

Fig. 5.2. Simulation BER, SESS-CD (64 chips/bit) and MRC, $K_{10} = K_{20} = K_{30} = 1; K_{12} = K_{13} = 1$.

in the middle of the source and destination (K_{12} = 0.5, K_{20} = 0.5) exhibits a better BER than the relay location near to the source (K_{12} = 0.9, K_{20} = 0.2). We can also see in Fig. 5.5 that SESS-CD is stable in correlated channels but MRC degrades rapidly as the channel correlation increases. A similar effect can be observed with bit loss in hostile channels as shown in Fig. 5.6 where SESS-CD displays much stable BER performance compared to the MRC.

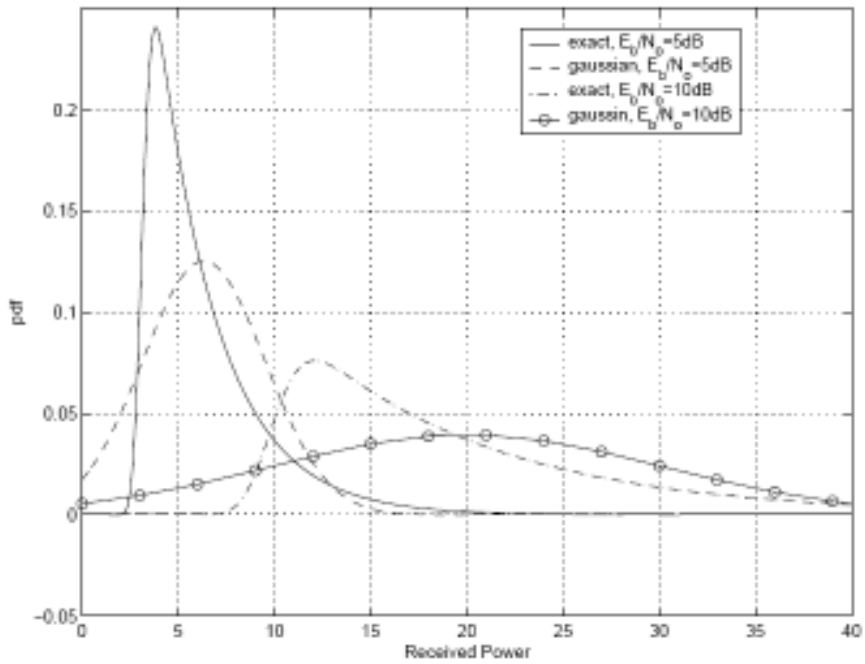

Fig. 5.3. Probability density function of exact pdf and Gaussian approximation, 64 chips/bit, *Eb/No* = 5 and 10 dB

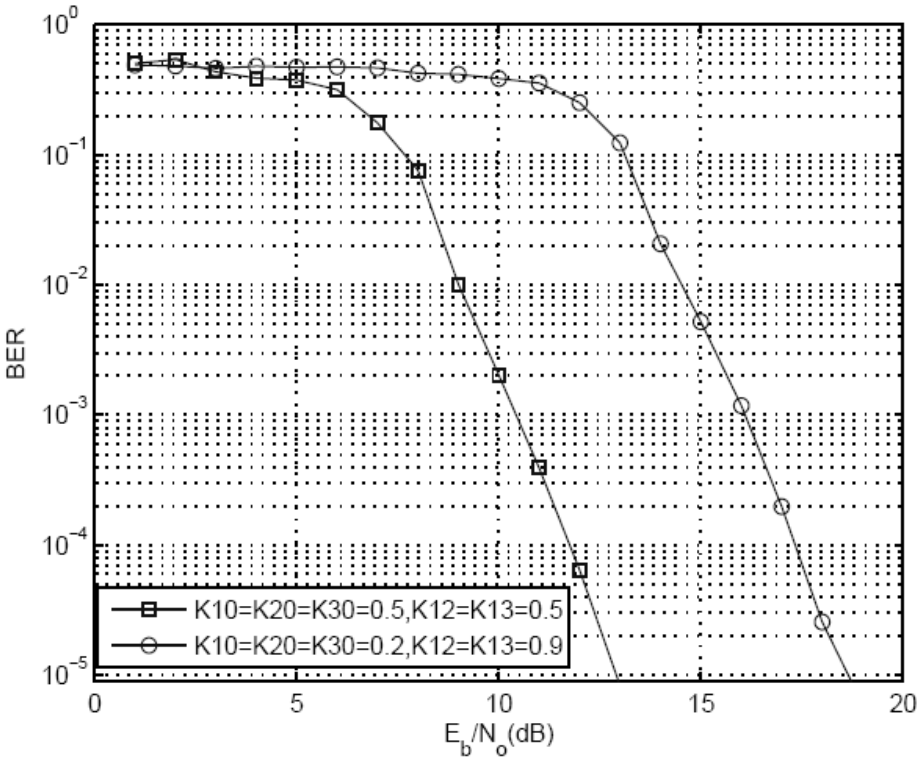

Fig. 5.4. Simulation BER of SESS-CD, 64 chips/bit.

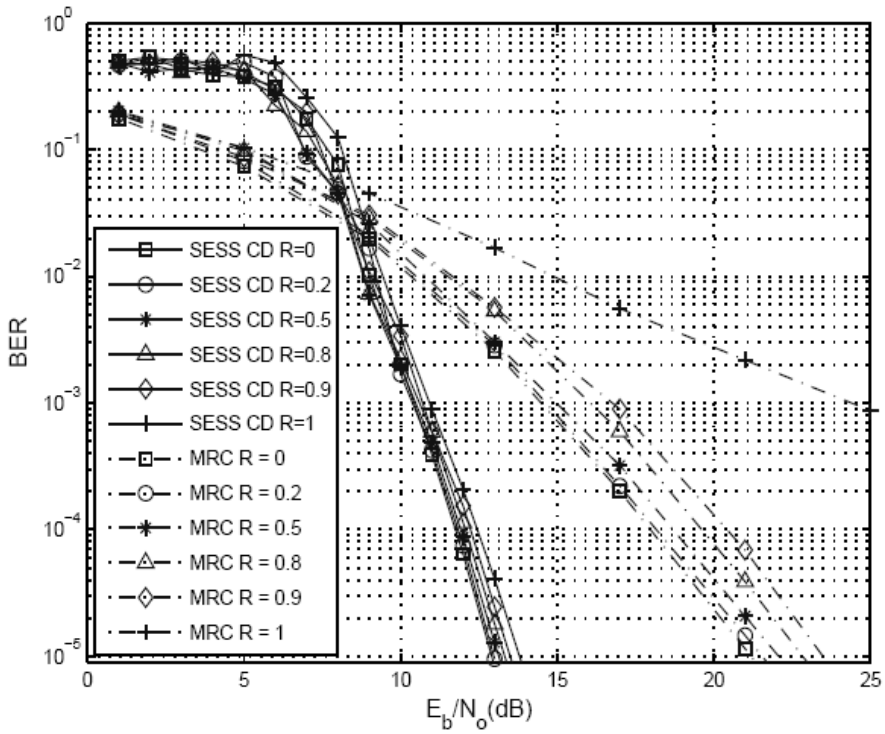

Fig. 5.5. Simulation BER of MRC and SESS-CD (64 chips/bit) with $K_{10} = K_{20} = K_{30} = 0.5$;$K_{12} = K_{13} = 0.5$, for various correlation values of correlated channel.

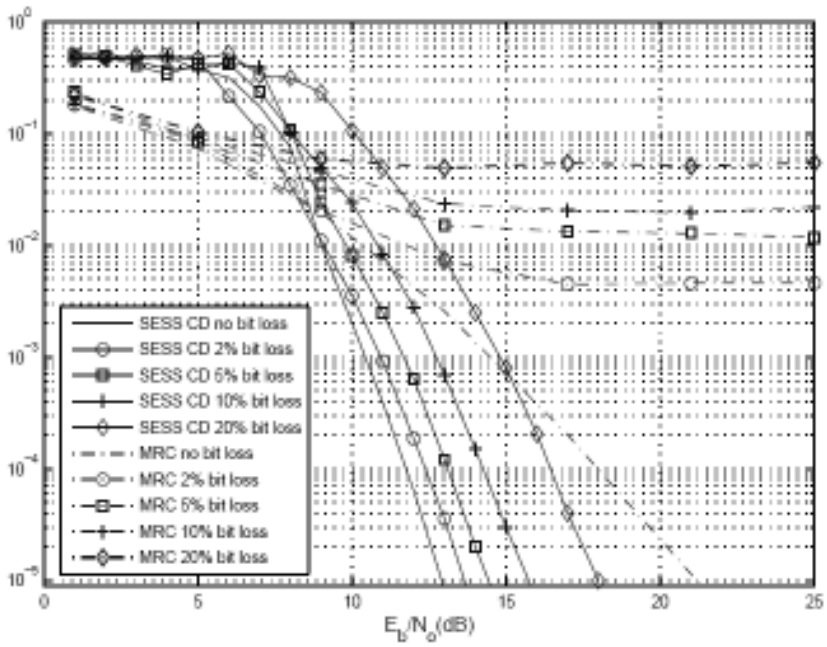

Fig. 5.6. Simulation BER of MRC and SESS-CD (64 chips/bit) with $K_{10} = K_{20} = K_{30} = 0.5, K_{12} = K_{13} = 0.5$, with various bit loss percentages.

5.5 Summary

In this chapter, we have incorporated SESS with CD and showed that SESS-CD diversity gain is related to the square of the received SNR: The BER of SESS-CD is inversely proportional to the square term of the SNR while the MRC BER is inversely proportional to the SNR only. The simulation results showed that SESS-CD is very stable in highly correlated channels as well as in severely fading channels. Thus SESS combined with CD can be a promising CD technique for the future generation of wireless communications.

CHAPTER 6
Concluding Remarks and Future Work

SESS and SEMA can be considered as low rate convolutional code or direct sequence random spread spectrum communications [16,48,49], they have some of the characteristic of channel coding as well as spread spectrum capability. SESS can achieve 3dB performance gain comparing to the conventional uncoded direct sequence spread spectrum system. As the spreading sequence is time variant and randomly generated, it has the potential to provide the system with low probability of interception. SESS is similar to a channel coding scheme in that it can also provide time diversity to combat against fading in wireless communication channel. Because of the large memory in SESS modulation, robust resistance of to time selective fading can be achieved without the explicit need of interleavers.

However, in SESS, the random and time-varying nature of self-encoded sequence presents a challenge to synchronization as no reference of the spreading sequence is available at the receiver. Thereby, a reliable acquisition and tracking system is critically important to SESS receiver. We consider the acquisition as a global optimization problem and propose to employ genetic search algorithm in the sequence generation and revision for converging to the global optimization efficiently.

(1) Synchronization time of SESS is necessary to be improved for the real application of SESS system. For example, for N=64, it will need around 150 bit periods on average to achieve the synchronization for SESS.

(2) The synchronization system we present assuming that system works under high SNR which can not always be promised in practical. Under low SNR, more noise will influence the quality of the estimation of transmitted signal in the receiver part.

(3) More parameters are necessary to evaluate the quality of SESS synchronization. For example, the acquisition probability in a fix time period, probability of false alarm, etc.

Some Improvements may have on Cooperative diversity:

(1) Synchronization

Cooperation diversity is assuming the whole system is well synchronized which is actually very hard in real application.

(2) Because the complexity in receiver is obviously increased by introducing cooperation diversity, Channel estimation and signal detection for cooperative diversity are necessary to be improved.

(3) Even multi-antennas are not applicable in transmitter users, but still suitable for base station. So a scheme of transmitting by cooperative diversity and receiving by multi-antennas diversity will be beneficial.

(4) Cooperation diversity in frequency selective fading channels. Untill now, most works on cooperation diversity are assuming system in flat fading channel. For high bit rate and high mobility communication system, the cooperation diversity research on frequency selective fading channels is necessary. Questions can be raised as: Can we transplant same results into frequency selective fading channels? What factors must be taken care in frequency selective fading channels? Barbarossa has been starting such work to combine cooperation diversity with OFDM, thereby, OFDM can be used to defeat frequency selective fading.

A novel scheme: SESS together with cooperative convolutional coding scheme and iterative detection can achieve both spatial and time diversity gain simultaneously without the average power increase. But the system will have much higher delay and computational complexity which need to be considered in the future. And the synchronization problem is critical for both SESS and CCC scheme, it's necessary to figure out a synchronization method for this novel SESS and CCC combination scheme.

Appendix A:

Examples of Simulink structures of SESS

1. Self-Encoding Feedback Detection (N=4,16,128,256,512,1024)

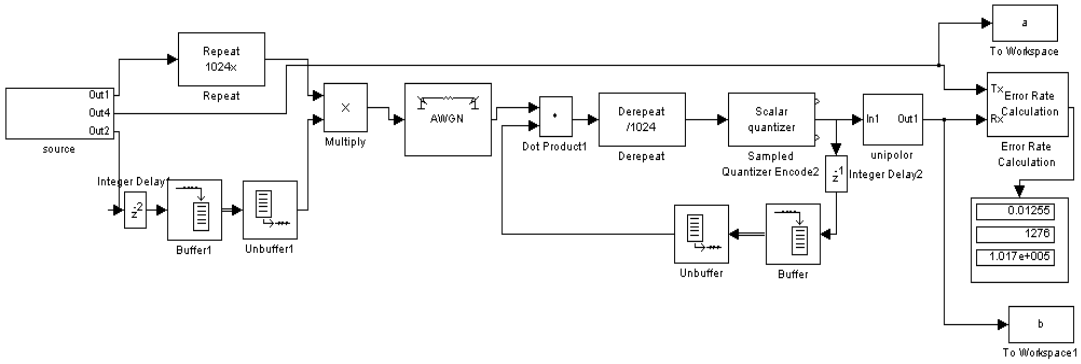

Fig A.1 Feedback Detection N=1024

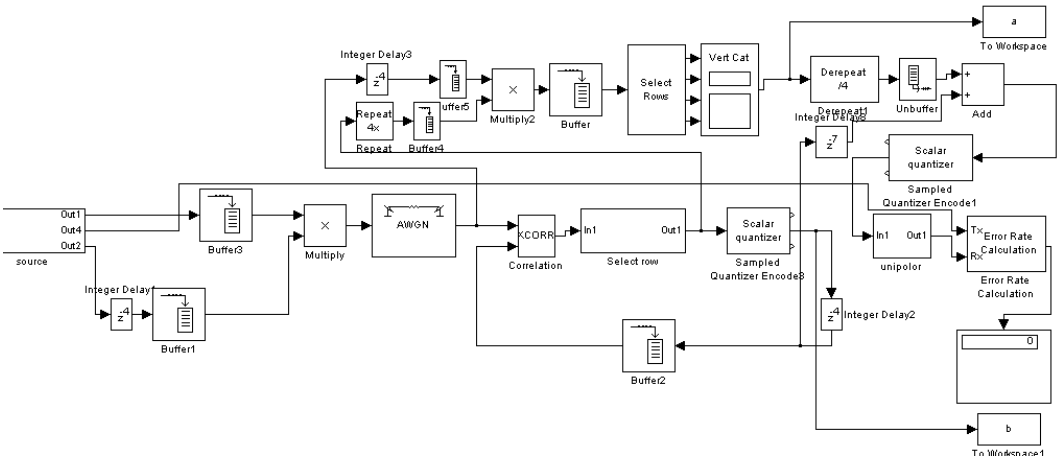

FigA.2 Iteration detection (N= 4,16,128,256,512)

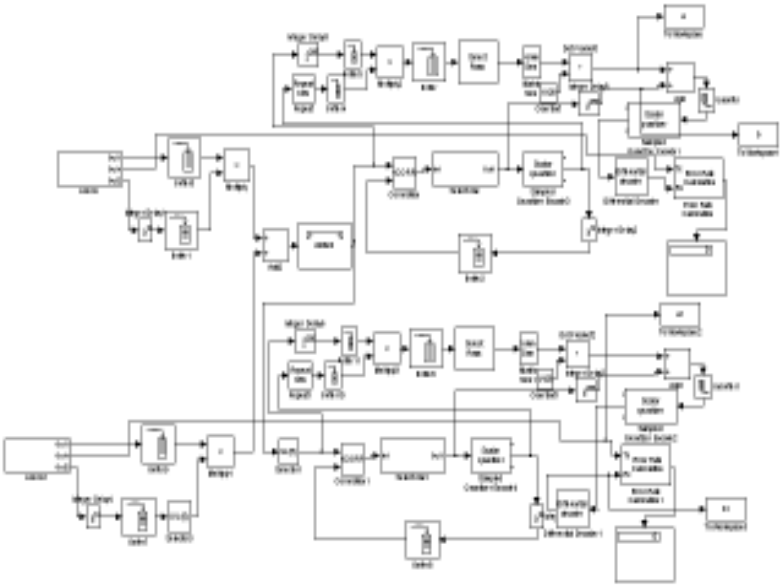

Fig.A.3 Self-Encoded Multiple Access for Iteration Detection (2 users)

Appendix B:

MPT Matrix M calculation codes (matlab)

```
N=16;
L=pow2(N);
Mo=zeros(L,L);
M_1=zeros(L,L);
Po=ones(1,L);
i=0;
I=eye(L);

P=zeros(L,L);
Perr=zeros(1,N+1);
for i=1:N+1
Perr(i)=normcdf((2*(i-1)/N-1)*sqrt(2));
end
%Perr=[0.08    0.1446    0.242    0.3632    0.5    0.6368    0.758    0.8554    0.92];          % N=8
%Perr=[0.08 0.242 0.5 0.758 0.92];                                                                % N=4


for i=1:L
    for j=1:L
        if i<=pow2(N-1)
            if i==ceil(j/2)

                ii=dec2binvec(i-1,N);

                tt=0;
                for k=1:N
                    if ii(k)==1
                        tt=tt+1;
                    end
                end

              if mod(j,2)==0
                P(i,j)=Perr(tt+1);
            else
                P(i,j)=1-Perr(tt+1);
            end

        end
```

```
        else
            if (i-pow2(N-1))==ceil(j/2)
                                        ii=dec2binvec(i-1,N);

                tt=0;
                for k=1:N
                    if ii(k)==1
                        tt=tt+1;
                    end
                end

              if mod(j,2)==0
                P(i,j)=Perr(tt+1);
            else
                P(i,j)=1-Perr(tt+1);
            end

            end
        end
    end
end

E=ones(L,L);
i=0;
M=E;
while (Mo~=M)
Mo=M;
M=E+P*(M-diag(diag(M)));
i=i+1;
disp(i);
end

Mmean=zeros(1,N+1);
Mnum=zeros(1,N+1);
for j=1:L
    jj=dec2binvec(j-1,N);
     tt=0;
     for k=1:N
        if jj(k)==1
            tt=tt+1;
        end
    end
      Mmean(tt+1)=Mmean(tt+1)+M(j,1);
      Mnum(tt+1)=Mnum(tt+1)+1;
```

```
end
Mm =Mmean./Mnum;
```

Appendix C:

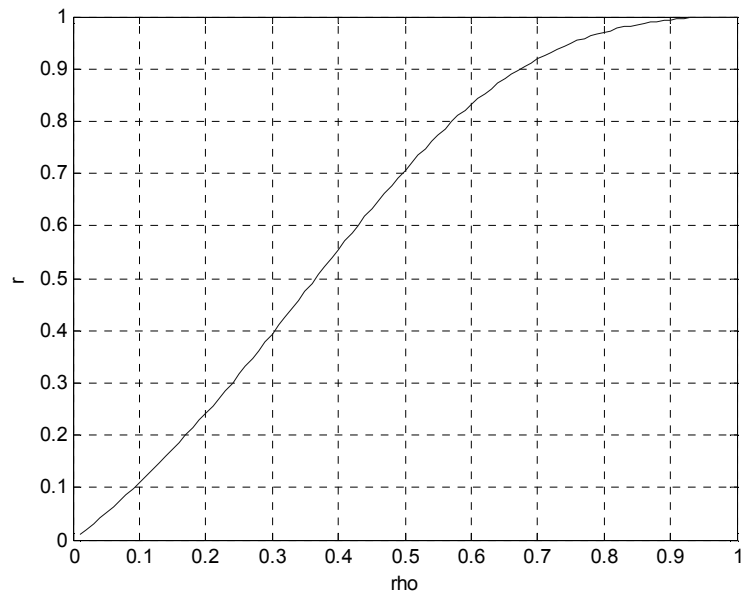

Fig. 4 Variance coefficient r with ρ for Chapter 4

Figure C.4 shows the relationship of r with ρ is nonlinear for correlated channels simulations in chapter 5. See detail deductions in next page.

Covariance Coefficient

$$\begin{aligned}
&\gamma[x_1x_2] = \frac{C(x_1x_2)}{\sqrt{C(x_1^2)C(x_2^2)}} \\
&C(x_1x_2) = R(x_1x_2) - E[x_1]E[x_2] \\
&R(x_1x_2) = E[x_1x_2] \\
&C(x_1x_2) = E[x_1x_2] - E[x_1]E[x_2]
\end{aligned} \tag{1}$$

Rayleigh Channel

$$\begin{aligned}
&E[x] = 1.2533\sigma = \sigma\sqrt{\tfrac{\pi}{2}} \\
&\sigma = \sqrt{\tfrac{2}{\pi}}E[X] \\
&C(x^2) = \tfrac{2}{\pi}(2 - \tfrac{\pi}{2})E^2[x] \\
&E[x^2] = C(x^2) + E^2[x] = \tfrac{4}{\pi}E^2[x]
\end{aligned} \tag{2}$$

$$P(r) = \begin{cases} \frac{r}{\sigma^2}exp(-\frac{r^2}{2\sigma^2}) & 0 \le r \le \infty \\ 0 & r < 0 \end{cases} \tag{3}$$

$x_2 = \rho x_1 + (1-\rho)x_3$ $\quad$ x_1 and x_3 are independent

$$\begin{aligned}
E[x_2] &= \rho E[x_1] + (1-\rho)E[x_3] \\
&= \rho E[x] + (1-\rho)E[x] \\
&= E[x]
\end{aligned} \tag{4}$$

$$\begin{aligned}
R(x_1x_2) &= E[x_1x_2] \\
&= E[x_1(\rho x_1 + (1-\rho)x_3)] \\
&= \rho E[x_1^2] + (1-\rho)E[x_1]E[x_3]
\end{aligned} \tag{5}$$

$$\begin{aligned}
C(x_1x_2) &= R(x_1x_2) - E[x_1]E[x_2] \\
&= \rho E[x_1^2] - \rho E[x_1]E[x_2] \\
&= (\tfrac{4}{\pi} - 1)E^2[x]\rho
\end{aligned} \tag{6}$$

$$\begin{aligned}
C(x_1^2) &= (\tfrac{4}{\pi} - 1)E^2[x] \\
C(x_2^2) &= E[x_2^2] - E[x_2]^2
\end{aligned} \tag{7}$$

$$\begin{aligned}
E[x_2^2] &= E[\rho^2x_1^2 + (1-\rho)^2x_3^2 + 2\rho(1-\rho)x_1x_3] \\
&= \rho^2E[x_1^2] + (1-\rho)^2E[x_3^2] + 2\rho(1-\rho)E[x_1]E[x_3] \\
&= \tfrac{4}{\pi}\rho^2 + (1-\rho)^2 + 2\rho(1-\rho)E^2[x]
\end{aligned} \tag{8}$$

$$\begin{aligned}
C(x^2) &= \tfrac{4}{\pi}(2\rho^2 - 2\rho + 1) - (2\rho^2 - 2\rho + 1)E[x]^2 \\
&= (\tfrac{4}{\pi} - 1)(2\rho^2 - 2\rho + 1)E[x]^2
\end{aligned} \tag{9}$$

$$\begin{aligned}
\gamma(x_1x_2) &= \frac{C(x_1x_2)}{\sqrt{C(x_1^2)C(x_2^2)}} \\
&= \frac{(\frac{4}{\pi}-1)E^2[x]\rho}{\sqrt{(\frac{4}{\pi}-1)E^2[x]\frac{4}{\pi}(2\rho^2-2\rho+1)E[x]^2}} = \frac{\rho}{\sqrt{2\rho^2-2\rho+1}}
\end{aligned} \tag{10}$$

$$\rho = \frac{\gamma}{\gamma + \sqrt{1-\gamma^2}} \tag{11}$$

References:

[1] O. Tero and P. Ramjee, *WCDMA: Towards IP Mobility and Mobile Internet,* Artech House, Boston, 2001

[2] R. A. Scholtz, "The Evolution of Spread-Spectrum Multiple-Access Communications," in *Code Division Multiple Access Communications*, Kluwer Academic Publishers, Boston, 1995.

[3] F. Ellersick, "A Conversation with Claude Shaanon," *IEEE Communications Magazine*, Vol. 22, No.5, pp.123-126 , May 1984.

[4] G. R. Cooper and R.W. Nettleton, "A Spread-Spectrum Technique for High-Capacity Mobile Communications," *IEEE Trans on Veh. Tech.*, Vol.27, No. 4, , pp. 264-275 , Nov. 1978.

[5] S. Verdu, "Minimum Probability of Error for Asynchronous Gaussian Multiple Access," *IEEE Trans. on IT*, Vol. IT-32, No.1 pp. 85-96, Jan. 1986,.

[6] A. Sendonaris, E. Erkip and B. Aazhang, "User Cooperation Diversity-Part I: System Description," *IEEE Trans on Commun.*, Vol. 51, No. 11, pp. 1927-1938, Nov.

2003.

[7] A. Sendonaris, E. Erkip E and B. Aazhang, "User Cooperation Diversity Part II: Implementation Aspects and Performance Analysis," *IEEE Trans on Commun.*, Vol. 51, No. 11, pp. 1939-1948, Nov. 2003.

[8] T. E. Hunter and A. Noosratinia, "Cooperative Diversity Through Coding," *Proc. IEEE Int. Symp. Inform. Theory*, Lausanne, Switzerland, pp. 220, Jun. 2002.

[9] M. Gastpar, G. Kramer and P. Gupta, "The Multiple-Relay Channel: Coding and Antenna-Clustering Capacity," Proc. *IEEE Int Symp Info Theory*, Lausanne, Switzerland, Jul. 2002.

[10] J. Boyer, D. Falconer, and H. Yanikomeroglu, "Cooperative connectivity models for wireless relaying networks," *WICAT Workshop on Cooperative Communications*, Oct. 2005.

[11] P. Gupta and P. R. Kumar, "The Capacity of Wireless Networks, " *IEEE Transactions on Information Theory,* vol. IT-46, no. 2, pp. 388-404, Mar. 2000.

[12] L. Nguyen, "Self-encoded spread spectrum and multiple access communication," *Proc. IEEE 6th Int. Symp. On Spread-Spectrum Techniques & Applications*, New

Jersey, Sep. 2000.

[13] Y. Kong, L. Nguyen and W. M. Jang, "Self-Encoded Spread Spectrum Modulation with Differential Encoding", *Proc. IEEE 7th Int. Symp. On Spread-Spectrum Techniques & Applications,* Prague, Czech Republic. Sep. 2002.

[14] J. S. Arora, O. A. Elwakeil, A. I. Chahande and C. C. Hsieh "Global optimization methods for engineering applications: A review," *Structural and Multidisciplinary Optimization,* Vol. 9, No. 3-4, Jul. 1995.

[15] W. M. Jang, L. Nguyen and M. Hempel, "Self-Encoded Spread Spectrum and Turbo Coding," *Journal of Communications and Networks,* Vol. 6 No. 1, pp. 9-18, Mar. 2004.

[16] Y. Kong, *Self-encoded Spread Spectrum and Multiple Access Communication Systems*, Dissertation Draft, University of Nebraska Lincoln, Dec. 2005

[17] W. M. Jang, L. Nguyen and M. Hempel, "Precoded Random Spreading Multiple Access in AWGN Channels," *IEEE Transactions on Wireless Commun.*, Vol. 3, No. 5, pp. 1477-1480, Sep. 2004.

[18] Y. S. Kim, W. M. Jang, Y. Kong and L. Nguyen, "Self-Encoded Multiple Access with Iterative Detection in Fading Channel," *Journal of Communications and Networks,* Vol. 9, No. 1, pp. 50-55, Mar. 2007.

[19] S. Sedghi, H. R. Mashhadi and M. Khademi "Detecting Hidden Information from a Spread Spectrum Watermarked Signal by Genetic Algorithm," *Proc. 2006 IEEE Congress on Evolutionary Computation,* Vancouver, BC, Canada, Jul. 16-21, 2006.

[20] W. J. Stewart, *Introduction to the Numerical Solution of Markov Chains*, Princeton University Press, New Jersey, 1994.

[21] A. Ribeiro, C. X. Cai and G. B. Giannakis, "Symbol Error Probabilities for General Cooperative Links," *IEEE Trans on Wireless Commun.*, Vol. 4, No. 3, pp. 1264-1273, May 2005.

[22] K. Hua, L. Nguyen and W.M. Jang, "Self-Encoded Spread Spectrum Synchronization with Genetic Algorithm and Markov Chain Analysis," Proc. *IEEE 42th Conference on Information Science and Systems*, Princeton, New Jersey, Mar. 2008.

[23] A. Ribeiro, X. Cai, and G. B. Giannakis, "Opportunistic Multipath for Bandwidth-Efficient Cooperative Networking," *Proc. IEEE Intnl. Conf. on Acoustics*

Speech and Signal Processing, Montreal, Canada, May 2004.

[24] S. Nagaraj and M. Bell, "A Coded Modulation Technique for Cooperative Diversity in Wireless Networks," *Proc. of IEEE International Conference on Acoustics, Speech, and Signal Processing* (ICASSP '05), Vol. 3, pp.525-528, Mar. 2005.

[25] N. J. Laneman and G. W. Wornell, "Distributed Space-Time-Coded Protocols for Exploiting Cooperative Diversity in Wireless Networks," *IEEE Trans. Inform. Theory*, Vol. 49, No. 10, pp. 2415-2425, Oct. 2003.

[26] Z. Wang and G. B. Giannakis, "A Simple and General Parameterization quantifying performance in fading channels," *IEEE Trans. Commun.*, Vol. 51, No. 8, pp. 1389-1398, Aug. 2003.

[27] M. Melanie, *An Introduction to Genetic Algorithms*, MIT Press, Cambridge, MA, 1996.

[28] G. R. Cooper, and C. D. McGillem, *Modern Communications and Spread Spectrum*, McGraw-Hill New York, 1986.

[29] R.C. Dixon, *Spread Spectrum Communications*, John Wiley & Sons, New York,

NY, 1984.

[30] E. Telatar, "Capacity of Multi-antenna Gaussian Channels," *AT&T Bell Laboratories, Tech.* Memo., Jun. 1995.

[31] P. S. Rossi, S.Yatawatta, A. P. Petropulu, F. Palmieri and G. Iannello, "A distributed coding cooperative scheme for wireless communications," *Signal Processing Advances in Wireless Communications,* 2005 IEEE 6th Workshop, pp 71 – 75, Jun. 2005

[32] Q. Yin and Y. Zhang, "Cooperative Diversity: A New Spatial Diversity Technique," Journal of Xi'an Jiaotong University, 552–557, Jun. 2005

[33] L.Nguyen, "Self-Encoded Spread Spectrum Communications," Proc. IEEE Military Communications Conference (*MILCOM 1999*), vol. 1, pp182-186, 1999.

[34] V. P. Ipatov *Spread Spectrum and CDMA*, John Wiley & Sons Ltd, The Atrium, Southern Gate, Chichester, West Sussex, England

[35] S. G. Glisic and B. Vucetic, *Spread Spectrum Cdma Systems for Wireless Communications.*

[36] M. Iosifescu, *Finite Markov Processes and Their Applications*, John Wiley & Sons, New York, 1980.

[37] D. Freedman, *Markov Chains*, Holden-Day, San Francisco, 1971.

[38] S.F. Alex, "Simulation of Genetic Systems by Automatic Digital Computers. I. Introduction". *Australian Journal of Biological Sciences* , pp 484-491.

[39] J. Laneman, D. Tse, and G. Wornell, "Cooperative Diversity in Wireless Networks: Efficient Protocols and Outage Behavior," *IEEE Trans. Inform. Theory*, vol. 50, no. 12, pp. 3062-3080, Dec. 2004.

[40] P. Frenger, P. Orten and T. Ottosson, "Convolutional Codes with Optimum Distance Spectrum", Proc. *IEEE Military Communications*, vol. 3,, pp. 317-319, 1999.

[41] T. Rappaport, *Wireless Communications Principle & Practice*, Prentice Hall, Upper Saddle River, NJ, 1996.

[42] A. J. Viterbi, "Error Bounds for Convolutional Codes and an Asymptotically Optimum Decoding Algorithm", *IEEE Transactions on Information Theory*, Volume IT-13, pp 260-269, Apr. 1967.

[43] Y. M. Kim and B. D. Woerner, "Comparison of Trellis Coding and Low Rate Convolutional Coding for CDMA," Proc. *IEEE MILCOM*, pp. 765-769, Forth Monmouth, NJ, 1994.

[44] W.M. Jang and L. Nguyen, "Capacity Analysis of Two User Self-Encoded Multiple Access System in AWGN Channels," *Proc. of 34th Annual Conference on Information Sciences and Systems,* Princeton, NJ, Mar. 2000.

[45] Z. Qin, K. C. Teh, and E. Gunawan, "Iterative Reduced-state Multiuser Detection for Asynchronous Coded CDMA," *IEEE Trans. Commun.* , vol. 50, no. 12, pp. 1892-1894, Dec. 2002.

[46] J. G. Proakis, *Digital communications*, 4th ed., McGraw-Hill, 2001.

[47] P. A. Anghel and M. Kaveh, "Exact Symbol Error Probability of A Cooperative Network in A Rayleigh-Fading Environment," *IEEE Trans on Wireless Commun.*, vol.3, no. 5, Sep 2004.

[48] P. Frenger, P. Orten, and T. Ottoson, "Code-Spread CDMA Using Low Rate Convolutional Codes," *Proc. IEEE Int. Symp. Spread Spectrum Techniques and Applications ,* pp. 374-378, 1998.

[49] S. Verdu and S, Shamai, "Spectral Efficiency of CDMA with Random

Spreading," *IEEE Trans. on Information Theory*, vol. 45, no. 2, pp. 622-640, Mar. 1999.

[50] W. C. Y. Lee, "Overview of Cellular CDMA," *IEEE Transaction on Vehicular Technology*, vol. 40, no. 2, May 1991.

[51] A. J. Viterbi, CDMA: *Principles of Spread Spectrum Communication,* Addison-Wesley, 1995

[52] S. Verdu, "Multiuser Detection", Cambridge University Press, Cambridge, 1998

[53] J. D. Parsons et. al., "Diversity Techniques for Mobile Radio Reception," *IEEE Trans. on Vehi. Tech.* , vol. VT-25, no. 3, pp. 75-84, 1976.

[54] S. Lin and D. J. Costello, *Error Control Coding: Fundamentals and Applications,* Prentice Hall, New Jersy, 1983

[55] T.R. Giallorenzi and S.G. Wilson, "Decision Feedback Multiuser Receivers for Asynchronous CDMA Systems," *Proc. of GLOBECOM'93*, pp. 1677-1681, Houston, TX, Nov-Dec. 1993.

[56] Z. Shi and C. Schlegel "Joint Iterative Decoding of Serially Concatenated Error Control Coded CDMA," IEEE JSAC. ,vol. 19, no 8, pp. 1646-1653, Apr.

2001.

[57] A. Duel-Hallen, “Multi-User Detection for CDMA systems,” *IEEE Pers. Commun.*, vol. 2, no. 2, pp. 46-58, Apr. 1995.

[58] S.D. Gray, M. Kocic and D. Brady “Multi-user Detection in Mismatched Multiple Access Channel,” *IEEE Trans. Commun.*, Vol. 43, no. 12, pp. 3080-3099, Dec. 1995.

[59] J. M. Holtzman, “A Simple, Accurate Method to Calculate Spread-Spectrum Multuple Access Error Probabilities,” *IEEE Trans. on Commun.*, vol. 40, no. 4, March 1992.

[60] Q. Li, X. Wang, and C. N. Georghiades, “Turbo Multiuser Detection for Turbo-coded CDMA in Multipath Fading Channels,” I*EEE Trans. Vehi. Tech*, vol. 51, no5, pp. 1096-1108, Sept. 2002.